After-effects of Parieto-occipital Gamma Transcranial Alternating Current Stimulation on Behavioral Performance and Neural Activity in Visuo-spatial Attention Task

Tianyi Zheng [1,*], **Yunshan Huang** [1], **Masato Sugino** [1], **Kenta Shimba** [2], **Yasuhiko Jimbo** [1] **and Kiyoshi Kotani** [2]

[1] *Department of Precision Engineering, The University of Tokyo, Tokyo, Japan*
[2] *Department of Human and Engineered Environmental Studies, The University of Tokyo, Chiba, Japan*

Correspondence*:
Corresponding Author
zheng@neuron.t.u-tokyo.ac.jp

ABSTRACT

Visuo-spatial attention enables selective focus on spatial locations while ignoring irrelevant stimuli which involves both endogenous and exogenous attention. Recent advancements in transcranial alternating current stimulation (tACS) have shown promise in modulating these attentional processes by targeting electrical oscillations in specific brain areas. Despite evidence of the online effects of tACS on the task performance of visuo-spatial attention, whether tACS can produce lasting after-effects on the behavioral performance and neural activity during the visuo-spatial attention task remains unknown. This study aims to explore these after-effects on visuo-spatial attention by implementing a single-blind, sham-controlled, between-group experiment design. Twenty young and healthy participants were equally divided into two groups receiving either sham or active gamma tACS at 40 Hz targeted at the right parieto-occipital region. Each participant engaged in a version of the Posner cueing task, conducted with EEG recording before and after the tACS intervention. The results revealed that the active tACS group exhibited significant reductions in reaction time compared to the sham group. These changes were not uniform across different attention types, suggesting specific enhancements in cognitive processing. Additionally, EEG analysis showed that gamma tACS influenced various aspects of neural activity, including event-related potentials to the target, as well as the oscillatory power and long-range temporal correlations of EEG signal during the cue-target interval. The amplitude and latency of N1 and P3 components were modulated by gamma tACS. Notably, there was a decrease in alpha power and an increase in gamma power during the cue-target interval, alongside a decrease in long-range temporal correlations. These findings revealed the after-effect of gamma tACS on modulating the behavioral performance and neural activity in the visuo-spatial attention task, paving the way for future applications in cognitive enhancement and therapeutic interventions.

Keywords: Transcranial alternating current stimulation (tACS), Visuo-spatial attention, Reaction time, Event-related potential (ERP), Neuronal oscillation, Long-range temporal correlations (LRTC), Electroencephalography (EEG)

1 INTRODUCTION

Visuo-spatial attention is a cognitive process that allows an individual to selectively concentrate on a specific spatial location within their visual environment while ignoring irrelevant stimuli thereby allocating limited cognitive processing resources to relevant information (Posner et al. (1980)). Visuo-spatial attention can be classified into two types: endogenous (top-down attention), and exogenous (bottom-up attention) (Corbetta and Shulman (2002)). Endogenous attention, also known as voluntary or goal-directed attention, is under the control of the individual and is directed by internal goals or intentions. Exogenous attention, on the other hand, is involuntary and is driven by external stimuli that are salient or stand out in some way, such as a bright flash or a sudden movement. Endogenous and exogenous attention can be assessed via variants of the Posner cueing task (Posner et al. (1980)) that measured subjects' reaction times to a visual target that appeared at expected (valid trial) or unexpected (invalid trial) following a central directional cue (endogenous cue) or a peripheral non-directional cue.

Empirical findings demonstrated that both types of visuo-spatial attention were regulated by neuronal oscillations in multiple frequency bands, including alpha oscillation (Klimesch (2012)) and gamma oscillation (Han et al. (2022)). Particularly, gamma oscillations in parietal and occipital cortex are crucial for visuo-spatial attention. Gamma oscillations in parietal region integrates sensory information from different modalities and is involved in the coordination of attention across spatial locations. Previous research has shown that gamma oscillations in the parietal cortex are essential for maintaining attention and processing spatial information (Gruber et al. (1999); Bosman et al. (2012)). Gamma oscillations in the occipital cortex have been linked to the enhancement of visual attention and the integration of visual stimuli (Magazzini and Singh (2018)). Stimulating the occipital cortex can modulate visual processing and improve attention-related tasks. Therefore, previous studies proposed non-invasive brain stimulation protocols induced electrical stimulation at a certain frequency to modulate neuronal oscillations and alter the capability of visuo-spatial attention (Reteig et al. (2017)).

Transcranial alternating current stimulation (tACS) is a non-invasive brain stimulation technique that applies oscillating electric fields to the brain through two or more electrodes placed on the scalp (Elyamany et al. (2021)). The electric current induced by tACS is of low intensity, typically lower than 4 mA peak-to-peak amplitude when applied to the scalp (Fröhlich (2014)). Studies applied online stimulation (subjects performing task while the tACS intervention), particularly in the frequency of alpha band (Kemmerer et al. (2022); Schuhmann et al. (2019); Radecke et al. (2023)) and gamma band (Kasten et al. (2020); Hopfinger et al. (2017)), achieved the improvement of accuracy and reduction of reaction time in visuo-spatial attention task, but not uniform across attention types. Parietal and occipital regions were commonly targeted in the tACS intervention due to their crucial roles in supporting visuo-spatial attention as evidenced by human and non-human studies (Bisley and Goldberg (2010); Somers and Sheremata (2013)). However, these studies primarily focused on the online effects of tACS during task performance. Whether gamma tACS can produce lasting after-effects on the behavioral performance of visuo-spatial attention remains unknown. Our study aims to investigate the after-effects of tACS by measuring task performance and neural activity before and after the stimulation, providing insights into the lasting impacts of tACS on visuo-spatial attention.

For the offline protocols (subjects performing task after the tACS intervention), the electrophysiological after-effect of alpha tACS was confirmed to last up to 70 min after stimulation in a visual attention task (Kasten et al. (2016)). Despite attentional functions, previous studies revealed after-effects of gamma tACS on working memory (Hoy et al. (2015)), motor learning (Giustiniani et al. (2019)), phonemic processing (Marchesotti et al. (2020)) and episodic memory recognition (Nomura et al. (2019)). Given the evidence

of significant role of gamma oscillations in visuo-spatial attention, online effects of gamma tACS in visuo-spatial attention, and its after-effects on other cognitive functions, we investigated the after-effect of parieto-occipital gamma tACS on behavioral performance and neural activity in a visuo-spatial attention task.

The study of the after-effects of tACS should include behavioral performance and neural activity. The current study utilized reaction time in a version of the Posner cueing task (Posner et al. (1980)) as the measurement of behavioral performance of visuo-spatial attention. Subjects were assigned to sham or active tACS groups with single-blind control. They were asked to perform the task once before and once after the sham or active tACS intervention, so that we could measure their performance change due to sham or active tACS.

To measure the neural activity, we used electroencephalography (EEG) to record the electrophysiological activity of the brain during the period when subjects performing the visuo-spatial attention task. We combined the analysis of event-related potential (ERP), oscillatory power of neuronal oscillations and long-range temporal correlations (LRTC) to capture a comprehensive picture of the neural mechanisms underlying the after-effects of gamma tACS on visuo-spatial attention. Event-Related Potentials (ERPs) are time-locked EEG responses to specific sensory, cognitive, or motor events. The analysis of ERPs can provide valuable information about the timing and amplitude of neural processes involved in visuo-spatial attention.

Experiments using EEG found the amplitude of visual event-related potential (Nakazono et al. (2020); Boetzel et al. (2023); Liu et al. (2023); Radecke et al. (2023)) were modulated by tACS and such modulation depends on the frequency of stimulation. In terms of behavioral performance, reaction time to the target was found correlated to the amplitude and latency of event-related potentials (Krieger and Dillbeck (1987); Kreegipuu and Allik (2007)). In this study, we are particularly interested in the changes in the N1 (90-200 ms after the onset of a stimulus) and P3 (250-400 ms after the onset of a stimulus) components evoked by the onset of target due to the after-effects of gamma tACS (Sur and Sinha (2009)). The N1 component is linked to early attention processing towards specific visual field locations (Di Russo et al. (2003)), while the P3 component indicates attentional resource allocation and cognitive processing speed (Chueh et al. (2017); Chang et al. (2015); Miniussi et al. (1999)). The enhancement of ERP components, such as increased amplitude of N1 and P3 components, happens when attention is directed to a specific spatial location. This enhancement indicates that the brain is allocating more resources to process stimuli at the attended location, thereby improving perceptual sensitivity and cognitive processing efficiency (Di Russo et al. (2003); Tendolkar et al. (2005)). On the other hand, changes in the latency of ERP components can indicate the speed of attentional processing. Shorter latencies typically suggest faster processing of attended stimuli, while longer latencies may indicate delayed processing (Di Russo et al. (2003)). The current study investigated the after-effect of gamma tACS on the amplitude and latency of event-related potentials which evoked by onset of target.

Further, neuronal oscillations refer to the rhythmic or repetitive neural activity in the brain. Analyzing these oscillations can reveal how neural synchrony and communication in certain regions or between different brain regions are modulated by tACS. As mentioned above, alpha and gamma bands oscillations supported the processing of visuo-spatial attention. Alpha oscillation were involved in the inhibition of irrelevant information (Klimesch (2012)) and attentional suppression (Foxe and Snyder (2011)) during the cue-target interval (CTI). The top-down attentional reorienting by frontal attention networks modulates gamma oscillatory activity in the primary motor cortex (M1) during movement execution (Spooner et al. (2020)) during CTI. Therefore, we expected that if offline gamma tACS could reduce reaction time in the

task, the alpha band power would decrease and the gamma band power would increase during CTI after tACS intervention.

Lastly, long-range-temporal correlations (LRTC) of EEG/MEG signals is a property observed in fluctuations of neural activity indicates the presence of temporal dependencies in the brain's oscillatory activity over extended time periods. Such fluctuations followed a power-law distribution, meaning that their statistical properties are scale-invariant over a wide range of time scales. Analysis of LRTC can provide insights into the scale-invariant, self-affinity temporal structure of neural activity, which was associated with behaviors and cognitive functions (Palva et al. (2013); Meisel et al. (2017); Sugimura et al. (2021)). The reaction time, that we utilized as a measurement of behavioral performance, has been demonstrated to correlate with the LRTC of neuronal oscillation (Irrmischer et al. (2018)), so we predicted that if offline gamma tACS could reduce reaction time in attention tasks the LRTC of EEG signal during CTI would be decreased in the cue-target interval.

To sum up, we hypothesized that the after-effects of active gamma tACS could improve the performance of a visuo-spatial attention task compared to the sham group, but may not be uniform across different attention types (trial types). Moreover, the event-related potential, oscillatory power, and long-range temporal correlations would be modulated by the intervention of active gamma tACS. To test our hypothesis, we designed a single-blind, sham-controlled, between-group experiment that assigned subjects to a sham or active tACS group and asked them to perform a visuo-spatial attention task once before and once after the sham/active tACS intervention. The EEG signal was recorded during the task to measure the neural activity altered by gamma tACS.

2 MATERIALS AND METHODS

2.1 Participants

Subjects were 20 healthy volunteers (4 females), ages 24.8 $\pm$ 2.0 years (M $\pm$ SD). None of the subjects had any history of neurological or psychiatric problems. All subjects had normal or corrected-to-normal visual acuity and no history of psychiatric illness, neurological disorder, or incident. Since caffeine, nicotine, and alcohol would influence brain dynamics (Vergara et al. (2018)), cognitive function (Lorist and Snel (1998)), and the effect of tACS (Antal et al. (2017)), subjects were asked to not take any of them within 24 hours before the experiment.

2.2 Procedure

Data were collected between January 2023 and July 2023 at The University of Tokyo, Japan. Prior to the experiment, the rationale and potential risk of the experiment, the potential side effects of tACS (e.g. slight tingling, burning, heat, and itching sensation over the scalp), and their right to withdraw at any time during the study were explained to the subjects.

The entire experiment was divided into three main sessions: a pre-tACS task, active or sham tACS, and a post-tACS task. We recorded the EEG signal of subjects during both pre-tACS task and post-tACS task sessions (Figure 1A). Subjects answered two questionnaires: one before the entire experiment and the other between the tACS session and the post-tACS task. The questionnaire before the entire experiment is to obtain information about age, sex, medical history, and ongoing medication. We also collected the input volume of caffeine, nicotine, and alcohol in the past month. The questionnaire answered after the tACS session is to report any tACS-induced sensations including itching, pain, burning, heat, metallic taste, fatigue, and general state.

Subjects sat on a comfortable chair throughout the entire experiment. We kept the laboratory quiet during two Posner cueing task sessions. During the process of answering questionnaires and tACS session, we kept the laboratory bright. During two Posner cueing task sessions, we kept the laboratory dim so that the subjects could easily see the visual target on the display.

2.3 Visuo-spatial attention task

The visuo-spatial attention task in the current study is a version of the Posner Cueing task (Posner et al. (1980)). We utilized reaction time in a Posner cueing task (Figure 1B) as a key metric to assess the visual attention of the subjects. Each task contained 120 trials. Each trial began with a fixation, during which subjects were asked to focus on a cross symbol at the center of the screen. Fixation was followed by the presentation of an endogenous cue or an exogenous cue, randomly presented to the subjects in 50-50 probability. The endogenous cue was a centered arrow located above the fixation cross pointing left or right with a 50-50 probability. The exogenous cue was a flashing box on the left or right side of the display with a 50-50 probability. Subjects were instructed to covertly shift their attention towards the cued location while focusing on a white central fixation cross, without rotating their eyeballs or moving their heads. To reduce precise timing expectancies, the cue-target interval (CTI) was set to T_{CTI} =0.5 or 1 second with 50-50 probability Hopfinger et al. (2017). After the random interval, a target was presented for a very short duration (0.05 seconds). The target appeared in the same direction as the cue in 80% of trials, which were valid trials, and in the opposite direction of the cue in 20% of trials, which were invalid trials. Subjects were instructed to respond by push a space key on a U.S. keyboard as soon as possible to the appearance of the target. The response period lasted for 1.5 seconds before the fixation of the next trial. The timing of the subjects pressing the key was recorded. The reaction time was defined as the duration from the onset of the target on the display until the subject pressed the button.

To increase the field of view and reduce visual fatigue (Park et al. (2017)), we used a curved display for the task(Figure 1C). Visual information was presented against a black background on a 49-inch curved display (Philips Brilliance 499P9H), with a resolution of 5120 $\times$ 1440, and a refresh rate of 60 frames per second. The plus symbol at the center of the display was for fixation. Two squares on the left and right sides of the fixation were the places where targets would appear. The target was disc-shaped (RGB = 1,0,0; 2° of visual angle). The target could appear in one of six possible locations inside the rectangular on the screen in order to reduce the predictability. All locations of targets shared the same probability. The six target locations were at the intersections of two horizontal trisects and three vertical quadrisects of the square on each side. The distance and angles in the panel were as follows: α=30°, β=10°, d=0.58 m. The length of each trial depends on the type of trial because the cue duration and cue-target interval (CTI) differ across types (Figure 1B). For trials with endogenous cue and short CTI interval (N=30), they were 4.55 s long. For trials with endogenous cues and long CTI (N=30), they were 5.05 s long. For trials with exogenous cues and short CTI (N=30), they were 3.682 s long. For trials with exogenous cues and long CTI (N=30), they were 4.182 s long. In total, one session of the visuo-spatial attention task took 523.92 s (8 min and 43.92 s).

2.4 Transcranial alternating current stimulation

Our montage of tACS selected 'P6' and 'Cz' of the international 10-20 system (Homan et al. (1987)) for electrode placement. The 10-20 system for electrode placement has been shown to reliably target desired cortex regions, including the parietal lobe (Herwig et al. (2003)). The location 'P6' is to stimulate the angular gyrus in the inferior parietal lobe, which is implicated in central mechanisms of movement perception and shifting of visual attention in the contralateral visual field (SAITO et al. (1992); Studer et al. (2014)). The 'Cz' electrode is positioned at the intersection of sagittal and coronal midlines, directing

the major electric field to the parieto-occipital regions. Moreover, a previous study found that online gamma tACS delivered at 'P6' and 'Cz' of the 10-20 system results in shortening the reaction time of endogenous trials of the Posner cueing task (Hopfinger et al. (2017)). Our montage of gamma tACS is to apply stimulation towards the parieto-occipital region which is crucial for visuo-spatial attention (Bisley and Goldberg (2010); Somers and Sheremata (2013)).

To understand which brain regions are affected by the tACS, we simulated the electric field of tACS using the ROAST package (Huang et al. (2019); roa (2018)) and New York head MRI structural image (Huang et al. (2016)). The majority of the electrical field induced by tACS affected the right parietal lobe and the right occipital lobe, as illustrated in Figure 1E. The concurrent stimulation of parietal and occipital regions was chosen based on their critical involvement in visuo-spatial processing (Gruber et al. (1999)) and the documented benefits of targeting these areas with gamma tACS (Hopfinger et al. (2017); Kasten et al. (2020)). While the simulation results indicate activation in a wide range of brain regions, including the temporal lobe and precentral gyrus, the primary focus remains on the parieto-occipital region. The broad activation can be attributed to the nature of tACS, which often affects multiple interconnected regions due to the diffuse nature of electric fields. However, the montage's main target remains in the parieto-occipital area, which aligns with our study's objectives.

Before the electrical stimulation, we applied skin preparation gel (skinPure, NIHON KOHDEN, Tokyo, Japan) to targeted areas of the subjects' scalp to reduce skin impedance. tACS was delivered by a battery-driven current stimulator (nurostym tES^{TM}, Neuro Device Group S.A., Warsaw, Poland) through two rubber carbon electrodes (Amrex CM-A102). Conductive paste (Ten20 paste, Weaver and Company, Aurora, CO) was applied to the electrodes to enable the electrodes to remain in place while allowing the transmittance of electrical signals. Two tACS electrodes (3×3 cm) were affixed to the location of 'P6' and 'Cz' of the 10-20 system using tape and supporting bandage. The impedance was kept below 10 kΩ during the stimulation session as monitored in real-time by the stimulator. The peak-to-peak amplitude and frequency of tACS were set to 1.5 mA and 40 Hz. The selection of 40 Hz as the stimulation frequency for tACS is based on its significance in gamma frequency, which is crucial for cognitive processing and sensory integration, enhancing neuronal synchronization and connectivity essential for processing complex visual stimuli and improving visuo-spatial attention (McDermott et al. (2018); Jia et al. (2011)). Additionally, 40 Hz stimulation has been shown to improve brain function through audiovisual (Chen et al. (2022)) and tACS interventions (Hopfinger et al. (2017)), positively impacting synaptic plasticity and brain network connections, thereby enhancing cognitive and attentional tasks. Since we intended to enhance the gamma band synchronization, subjects received in-phase 40 Hz tACS, that phase difference was 0° between 'P6' and 'Cz', for the tACS intervention (ten Oever et al. (2016); Abellaneda-Pérez et al. (2020)). The active stimulation included a fade-in and fade-out of 10 seconds each and a main stage duration of 15 minutes. The sham stimulation ramped up to 1.5 mA and ramped down to 0 in 10 seconds of both the fade-in and fade-out stages. In the main stage, the sham stimulation delivered brief pulses of 2 cycles of tACS at 0.6 mA, 40 Hz every 500 ms.

Current study was sham-controlled and single-blinded which enables us to eliminate the placebo effect of stimulation (Romanella et al. (2023); Braga et al. (2021)). Subjects were randomly assigned to either the sham stimulation group (N=10) or the active stimulation group (N=10) and were unaware of which group they belonged to. To assess blinding success, a blinding survey was completed at the end of the tACS session by asking subjects to guess whether they received active or sham stimulation. The information of reported group and conditioned group were collected in Table 1. We observed that subjects were unable to guess at better than chance level whether they had received an active or sham tACS (McNemar's test,

χ^2=1.778, p=.182). Stimulation was well tolerated, with only mild and transient side effects reported (e.g. itching and pain sensation close to the electrode, and phosphene perception).

2.5 EEG data acquisition

We recorded EEG signals during two Posner cueing task sessions. The EEG recording system included: two EEG amplifiers (g.USBamp), two driver (interface) boxes for active electrodes (g.GAMMAbox), an elastic EEG cap (g.EEGcap), and 32 active electrodes (g.ACTIVEelectrode, Ag/AgCl), one ground electrode (g.ACTIVEground, Ag/AgCl), and one reference ear clip (g.GAMMAearclip, Ag/AgCl). All components were manufactured by g.tec Medical Engineering GmbH, Schiedlberg, Austria. Conductive gel (g.GAMMAgel, g.tec Medical Engineering GmbH, Schiedlberg, Austria) was applied to the electrodes. Electrodes were mounted according to the international 10-20 system (Figure 1D) with A1 on the left ear as a common reference and Fpz on the forehead as a common ground. We used a microcontroller board (Arduino Uno, arduino.cc) to send a trigger signal from the computer for Posner cueing task to the EEG amplifier. EEG data were digitized at a sampling rate of 1200 Hz with a band-pass filter between 0.1 and 100 Hz and a notch filter at 50 Hz (48-52 Hz, to remove power line interferences). We use MATLAB Simulink to acquire EEG data from EEG amplifiers (Documentation (2020)).

2.6 Data processing and statistics

2.6.1 Behavior data

Our statistical analyses on behavior data were conducted using Python, utilizing libraries including NumPy (Harris et al. (2020)), pandas (McKinney et al. (2010)), SciPy (Virtanen et al. (2020)) and statsmodels (Seabold and Perktold (2010)). Analysis of reaction times was performed on correct responses. Early responses that were too fast to reflect genuine reactions (<100ms after target onset), as well as extremely slow reaction times (>1s after target onset) were removed. These rejections resulted in a loss of 5.3%$\pm$1.1% (M $\pm$ SD) of trials per subject. We categorized all trials into four types based on the cue-target combinations: endogenous cue followed by a valid target (Endo-Valid), endogenous cue followed by an invalid target (Endo-Invalid), exogenous cue followed by a valid target (Exo-Valid), and exogenous cue followed by an invalid target (Exo-Invalid). We used Shapiro-Wilk test to examine the normality of reaction times (Shapiro and Wilk (1965)). The normality of the entire reaction time dataset, the Endo-Valid dataset, the Endo-Invalid dataset, the Exo-Valid dataset and the Exo-Invalid dataset all achieved p>0.05. Therefore, the null hypothesis, that the data came from a normally distributed population, can not be rejected. We performed a three-way repeated-measures analysis of variance (ANOVA) with two within-subject factors: task times (pre-/post- tACS tasks), and trial types (Endo-Valid, Endo-Invalid, Exo-Valid and Exo-Invalid); and one between-subject factor: groups (sham/active groups) (Mashal and Metzuyanim-Gorelick (2019); Du et al. (2022); Imbert et al. (2022)). Later, two-way repreated-measures analysis of variance (ANOVA) with task times (pre-/post- tACS tasks) as within-subject factor and groups (sham/active groups) as between-subject factor was performed to each type of trials. Further exploratory analysis was carried out using post hoc t-tests with a Bonferroni correction (Armstrong (2014)) to investigate the pairwise difference of reaction time between pre- and post- tACS as well as between sham and active groups.

2.6.2 EEG Preprocessing

The preprocessing and further analysis of EEG signals were performed using Python, including MNE-Python (Gramfort et al. (2013)), NumPy (Harris et al. (2020)), pandas (McKinney et al. (2010)), and SciPy (Virtanen et al. (2020)) libraries. The continuous EEG data were epoched by trials, from the onset of

fixation to the end of the response stage. EEG epochs holding no responses or incorrect responses rejected by behavior data were removed. To clear the EEG data from artifacts like muscle, heart, eye blinks and eye movements, the remaining trials were fed into an independent component analysis (ICA) using a Picard method (Ablin et al. (2018)). We decomposed 32 independent components and manually rejected 6.2 $\pm$ 1.4 components (M $\pm$ SD) by screening topography, epochs image, event-related potential, power spectrum, and epoch variance of those components. These components were rejected due to muscle activity, eye blinks, heartbeats, and other noise artifacts that were identified in the screening. Finally, the data were re-referenced to the common average reference.

2.6.3 Event-related potential (ERP) analysis

For the ERP analysis of the EEG data, we applied a low-pass filter at 30 Hz to the epoched EEG data (Zhang et al. (2023)) to remove high-frequency components, followed by a linear detrend procedure. EEG data for ERP analysis were then epoched to a 0.6 s period in each trial (-0.1 to 0.5 s, relative to the onset of target on the screen) and baseline-corrected with respect to -0.1 to 0 s. We chose electrodes on the parieto-occipital sites in the study of ERP, including Pz, P5, P6, P7, P8, PO3, PO4, O1, and O2. The choice of specific electrodes for ERP analysis in visuo-spatial attention tasks is supported by studies that have localized ERP components to the parietal and occipital cortices (Hillyard and Anllo-Vento (1998); Di Russo et al. (2003); Eimer (1999)). These electrodes were chosen because they were typically used in the ERP analysis of visuo-spatial attention tasks (Thut et al. (2006); Zani et al. (2020); Sadeghi and Nazari (2015); Szewczyk et al. (2022)). We performed a three-way repeated-measures analysis of variance (ANOVA) with two within-subject factors: task times (pre-/post- tACS tasks), and trial types (Endo-Valid, Endo-Invalid, Exo-Valid and Exo-Invalid); and one between-subject factor: groups (sham/active groups) (Mashal and Metzuyanim-Gorelick (2019); Du et al. (2022); Imbert et al. (2022)). Later, mean amplitudes for each group, task time, and trial type were computed across selected electrodes. The statistical significance of amplitude change in different task times was measured by paired t-tests (pre-tACS task vs. post-tACS task). The multiple comparisons across time were controlled by the false discovery rate (FDR; Benjamini and Hochberg (1995)).

2.6.4 Oscillatory power analysis

For the computation of the oscillatory power of neuronal oscillations, we initially applied a linear detrend procedure to the epoched preprocessed EEG data. All channels were used in the analysis of oscillatory power as well as the long-range temporal correlations afterward. The rationale for using all EEG electrodes is based on findings that changes in these indexes can occur across large regions of the brain, spanning several lobes (Fingelkurts and Fingelkurts (2014); Morales and Bowers (2022); Nakao et al. (2019)). EEG data for band power analysis were then epoched to the CTI stage for each trial (from the disappearance of cue to the onset of target). Due to two lengths of CTI (T_{CTI} =0.5 or 1s) in the task setting, the length of epoched data was also 0 to 0.5 s, or 0 to 1 s, relative to the disappearance of the cue. We analyzed two frequency bands: alpha (8-12 Hz) and gamma (30-45 Hz). The aperiodic signal follows a 1/f-like distribution that spectral power decreases exponentially with increasing frequencies. The mean of EEG data was subtracted from each segment before computing its power spectral density (PSD). We employed a multitaper method in the MNE-Python package to compute the PSD of EEG data with DPSS tapers (Slepian (1978); Babadi and Brown (2014)). The frequency bandwidth of the multitaper window function was $8/T_{CTI}$, where $T_{CTI} = 0.5$ or 1 s for two lengths of CTI, respectively. Only tapers with more than 90% spectral concentration within bandwidth were used in the computation. The oscillatory powers of each frequency band were then computed by integrating PSD values over respected bands. Further, we

measured the effects of tACS on oscillatory powers via non-parametric cluster-based permutation analysis in the MNE-Python package. This method allowed the examination of global changes in band power across all EEG electrodes while controlling multiple comparisons, which has been used in previous studies investigating the effect of transcranial electrical stimulation on oscillatory power (Davis et al. (2023); Murphy et al. (2020)). Clusters in the current study were defined as two or more adjacent electrodes at a $p<0.05$ in t-tests with identical sign of t-values (i.e. all positive or all negative). We used a Monte Carlo method with 2000 iterations subsequently to calculate the two-tailed significance probability. The statistical analysis of the electrode cluster with significant change was carried out using post hoc t-tests with a Bonferroni correction (Armstrong (2014)) to investigate the pairwise difference of oscillatory power between pre- and post- tACS as well as between sham and active groups.

2.6.5 Detrended fluctuation analysis (DFA)

To quantify the long-range temporal correlations of EEG signals, we employed Detrended Fluctuation Analysis (DFA). DFA allowed us to compute the α-value of a segment of EEG signal, an index reflecting the presence and strength of LRTC in neural activity. In this study, we adhered to the methodology described by Peng et al. (1994), utilizing the fathon Python library for computational purposes (stfbnc and Katz (2023)). Our detrended fluctuation analysis (DFA) was specifically applied to EEG signals obtained during two stages: the CTI following endogenous cues, and the CTI following exogenous cues. The preprocessed EEG data was epoched to CTI of each trial. The length of epochs were dependent on the length of CTI as $T_{CTI} = 0.5$ or 1 s, respectively. The EEG signal, as a discrete time series, was denoted as $x(i), 1 \leqslant i \leqslant N$. The initial step in DFA involved subtracting the mean from the time series and then integrating the time series as follows

$$y(k) = \sum_{i=1}^{k}[x(i) - \langle x \rangle], 1 \leqslant k \leqslant N, \tag{1}$$

where $\langle x \rangle$ represents the average of the time series over the range $[1, N]$. Next, we divide $y(k)$ into contiguous segments with length n (n denotes the time scale of observation, $25 \leqslant n \leqslant 200$). For each segment, the local trend is determined by least-squares fit. The ensuing piece-wise linear fit is denoted as $y_n(k)$. Then, the integrated time series $y(k)$ is detrended by subtracting the local linear trend $y_n(k)$ for each segment. The root-mean-square fluctuation of this integrated and detrended time series is then computed by

$$F(n) = \sqrt{\frac{1}{N}\sum_{k=1}^{N}[y(k) - y_n(k)]^2}. \tag{2}$$

Next, the computation of $F(n)$ is repeated for a range of different scales n. In the final step, the logarithm of $F(n)$ against the logarithm of the time scale n is plotted. If the time series $x(i)$ has self-affinity, and scale-free fractal properties, the resulting plot will display a linear region with a certain slope. This slope, denoted as α, in the linear part of the plot of $\log(F_n)$ versus $\log(n)$, is called scaling exponent as

$$F(n) \propto n^{\alpha}. \tag{3}$$

Further, we measured the effects of tACS on LRTC (α-value) via non-parametric cluster-based permutation analysis in the MNE-Python package. This method allowed the examination of global changes in α-value across all EEG electrodes while controlling multiple comparisons. Clusters in the current study were defined as two or more adjacent electrodes at a $p<0.05$ in t-tests with identical sign of t-values (i.e. all

positive or all negative). We used a Monte Carlo method with 2000 iterations subsequently to calculate the two-tailed significance probability. The statistical analysis of the electrode cluster with significant change was carried out using post hoc t-tests with a Bonferroni correction (Armstrong (2014)) to investigate the pairwise difference of oscillatory power between pre- and post- tACS as well as between sham and active groups.

3 RESULTS

3.1 Reaction time is more reduced in post-active stimulation than post-sham stimulation

Reaction times for correct trials were first submitted to a 2x2x4 repeated-measures ANOVA, with factors of group, task time, and trial type. The omnibus analysis resulted in significant main effects of group (F(1,18)=19.26, p<.01, η_p^2=0.037), task time (F(1,18)=52.12, p<.01, η_p^2=0.104), and trial type (F(3,54)=118.3, p<.01, η_p^2=0.751). Moreover, there was a significant two-way interaction of group x task time (F(1,18)=24.72, p<.01, η_p^2=0.047). No significant main effect was observed in two-way interactions of group x trial type (F(3,54)=1.14, p=.34, η_p^2=0.006, or task time x trial type (F(3,54)=2.35, p=.08, η_p^2=0.014). The three-way interaction of group x task time x trial type was also not significant (F(3,54)=1.87, p=.15, η_p^2=0.012). The three-way repeated-measures ANOVA represented that the reaction times were significantly influenced by the group, task time, and trial type, with a notable interaction between group and task time. This indicated that sham and active tACS intervention result in varied reaction time in post-tACS task compared to pre-tACS task. Due to the large effect size for the trial type, and the evidence that attention types (Dugué et al. (2020)) and cue validity (Dugué et al. (2017); Osaki et al. (2021)) had a significant impact on reaction time, we separated the analysis of each trial type and further studied the interaction between group and task times for each trial type (Figure 2).

For the 2x2 repeated-measures ANOVA of Endo-Valid trials, main effects of group (F(1,18)=9.07, p<.01, η_p^2=0.194) and task time (F(1,18)=16.98, p<.01, η_p^2=0.378) were significant. The main effect of two-way interaction of group x task time was also significant (F(1,18)=4.78, p=.04, η_p^2=0.095). To further examine the effects of sham and active tACS on reaction time, we conducted a pairwise comparison among the reaction time in pre-sham, post-sham, pre-active and post-active tasks (Figure 2A). Pairwise t-tests confirmed the reaction time reduction in the sham group was significant (p=.02), from 334.7 $\pm$ 51.4 ms (M $\pm$ SD) in the pre-sham task to 329.5 $\pm$ 67.2 ms in the post-sham task. The reaction time reduction in the active group was also significant (p<.01), from 334.1 $\pm$ 80.3 ms in the pre-active task to 311.2 $\pm$ 60.8 ms in the post-active task. Moreover, the reaction time in the post-active task was significantly lower than in the post-sham task (p=.03).

For the 2x2 repeated-measures ANOVA of Endo-Invalid trials, main effects of group (F(1,18)=6.88, p=.02, η_p^2=0.179) and task time (F(1,18)=11.72, p<.01, η_p^2=0.316) were significant. The main effect of two-way interaction of group x task time was also significant (F(1,18)=5.22, p<.03, η_p^2=0.136). Pairwise t-tests (Figure 2B) confirmed the reaction time reduction in the sham group was not significant (p>.05), from 428.8 $\pm$ 94.1 ms in the pre-sham task to 419.1 $\pm$ 86.0 ms in the post-sham task. However, the reaction time reduction in the active group was significant (p=.01), from 422.0 $\pm$ 125.8 ms in the pre-active task to 388.4 $\pm$ 86.6 ms in the post-active task. Moreover, the reaction time in the post-active task was significantly lower than in the post-sham task (p<.01).

For the 2x2 repeated-measures ANOVA of Exo-Valid trials, main effects of group (F(1,18)=12.57, p<.01, η_p^2=0.148) and task time (F(1,18)=39.51, p<.01, η_p^2=0.481) were significant. The main effect of two-way interaction of group x task time was also significant (F(1,18)=16.75, p<.01, η_p^2=0.202). Pairwise t-tests

(Figure 2C) confirmed the reaction time reduction in the sham group was significant (p=.01), from353.3 ± 67.0 ms in the pre-sham task to 343.9 ± 80.7 ms in the post-sham task. The reaction time reduction in the active group was also significant (p<.01), from 357.6 ± 109.3 ms in the pre-active task to 312.3 ± 75.7 ms in the post-active task. Moreover, the reaction time in the post-active task was significantly lower than in the post-sham task (p<.01).

For the 2x2 repeated-measures ANOVA of Exo-Invalid trials, the main effects of neither group (F(1,18)=0.03, p=.86, η_p^2=0.001) nor task time (F(1,18)=1.86, p=.19, η_p^2=0.114) were significant. The main effect of two-way interaction of group x task time was also not significant (F(1,18)=0.49, p=.49, η_p^2=0.031). Although the mean reaction time reduced from 373.8 ± 68.8 ms to 361.6 ± 63.5 ms in the sham group and from 372.2 ± 90.5 to 366.0 ± 88.4 ms in the active group, pairwise t-tests (Figure 2D) revealed no significant difference among groups and task times (all p>.05). These results suggested that the after-effect of our stimulation protocol on reaction time was not uniform across trial types. Task performance in Endo-Valid, Endo-Invalid, and Exo-Valid trials represented significant enhancement after the active intervention of gamma tACS but not in Exo-Invalid trials.

3.2 Diverse after-effects of active tACS on event-related potentials across trial types

Event-related potentials of correct trials in the time window of N1 component, which is 90-200 ms after the onset of a stimulus, and P3 component, which is 250-400 ms after the onset of a stimulus (Sur and Sinha (2009)) were first submitted to a 2x2x4 repeated-measures ANOVA. For the ANOVA of ERP in the time window of N1 component, the omnibus analysis resulted in significant main effects of group (F(1,18)=6.71, p=.02, η_p^2=0.111), task time (F(1,18)=21.14, p<.01, η_p^2=0.141), and trial type (F(3,54)=39.04, p<.01, η_p^2=0.356). Moreover, there was a significant two-way interaction of group x task time (F(1,18)=22.74, p<.01, η_p^2=0.187). No significant main effect was observed in two-way interactions of group x trial type (F(3,54)=1.41, p=.25, η_p^2=0.003), or task time x trial type (F(3,54)=1.12, p=.35, η_p^2<0.001). However, the three-way interaction of group x task time x trial type was significant (F(3,54)=3.04, p=.04, η_p^2=0.091). For the ANOVA of ERP in the time window of P3 component, the omnibus analysis resulted in significant main effects of group (F(1,18)=19.38, p<.01, η_p^2=0.086), task time (F(1,18)=58.62, p<.01, η_p^2=0.373), and trial type (F(3,54)=38.90, p<.01, η_p^2=0.087). Moreover, there were significant two-way interaction of group x task time (F(1,18)=22.85, p<.01, η_p^2=0.130), and task time x trial type (F(3,54)=3.22, p=.03, η_p^2=0.096). No significant main effect was observed in two-way interactions of group x trial type (F(3,54)=0.97, p=.41, η_p^2=0.005). However, the three-way interaction of group x task time x trial type was significant (F(3,54)=3.14, p=.03, η_p^2=0.033).

The three-way repeated-measures ANOVA found complex interplay between factors including group, task time and trial type. Combining with the analysis of reaction time showed significant reductions in reaction time observed in Endo-Valid, Endo-Invalid, and Exo-Valid trials, not Exo-Invalid (Figure 2), we separated the analysis of ERP into those four trial types. We compared the difference in ERP between pre-sham vs. post-sham as well as pre-active vs. post-active tasks to investigate the after-effect of sham-active tACS. Analysis of ERP revealed diverse after-effects of active-tACS across trial types in the post-active task compared with the pre-active task (Figure 3).

For Endo-Valid trials, no significant difference in ERPs was observed between pre-sham and post-sham tasks, but significant differences were observed in ERPs of the active group. From 128 ms to 163 ms after the target onset, which fell into the latency of the N1 component, post-active ERP showed less negative deflection than pre-active ERP (Figure 3A). For Endo-Invalid trials, no significant difference in ERPs was observed between pre-sham and post-sham tasks, but significant differences were observed in two ERP

segments of the active group. From 330 ms to 340 ms after the target onset and from 368 ms to 405 ms, which fell into the latency of the P3 component, post-active ERP showed shorter latency than pre-active ERP (Figure 3B).

For Exo-Valid trials, no significant difference in ERPs was observed between pre-sham and post-sham tasks, but significant differences were observed in two ERP segments of the active group. From 261 ms to 267 ms after the target onset and from 323 ms to 344 ms, which fell into the latency of the P3 component, post-active ERP showed shorter latency than pre-active ERP (Figure 3C). Finally, for Exo-Invalid trials, we observed no significant difference in ERPs between neither pre-sham vs. post-sham nor pre-active vs. post-active (Figure 3D). Our findings represented non-uniform after-effects of gamma tACS on ERPs across trial types. Significant changes in the amplitude of N1 components as well as amplitude and latency of P3 components were observed in Endo-Valid, Endo-Invalid, and Exo-Valid trials but not in Exo-Invalid trials which aligns with our findings of reaction time.

3.3 Decreasing of oscillatory power in alpha band but increasing in gamma band during CTI after active-tACS intervention

Further, we investigated the after-effects of gamma tACS on the oscillatory power during CTI period. Due to different roles of alpha and gamma oscillations as well as different mechanism of endogenous and exogenous attention (Riddle et al. (2019)), we separate the analysis of oscillatory power as frequency band x trial type, result in four combinations. For the oscillatory power in the alpha band in CTI following endogenous cue, non-parametric cluster-based permutation analysis revealed a significant decrease over the right hemisphere (pre-active vs. post-active, $p=.021$), while no significant difference was observed in comparisons of neither pre-sham vs. pre-active nor pre-sham vs. post-sham (Figure 4A, topographical maps). We further measured the average oscillatory power of electrodes in the significant cluster. As shown in the bar plot of Figure 4A, we found the alpha power in the significant cluster was significantly decreased after active-tACS ($p=.03$) and the alpha power was significantly lower in the post-active task than post-sham task ($p<.01$) (pre-sham vs. post-sham, pre-sham vs. pre-active, all $p>.05$).

For the oscillatory power in the alpha band in CTI following exogenous cue, non-parametric cluster-based permutation analysis revealed a significant decrease over the right hemisphere (pre-active vs. post-active, $p=.017$), while no significant difference was observed in comparisons of neither pre-sham vs. pre-active nor pre-sham vs. post-sham (Figure 4B, topographical maps). We further measured the average oscillatory power of electrodes in the significant cluster. As shown in the bar plot of Figure 4B, we found the alpha power in the significant cluster was significantly decreased after active-tACS ($p=.04$) and the alpha power was significantly lower in the post-active task than post-sham task ($p=.02$) (pre-sham vs. post-sham, pre-sham vs. pre-active, all $p>.05$).

For the oscillatory power in the gamma band in CTI following endogenous cue, non-parametric cluster-based permutation analysis revealed a significant increase over the frontal and central sulcus regions (pre-active vs. post-active, $p=.004$), while no significant difference was observed in comparisons of neither pre-sham vs. pre-active nor pre-sham vs. post-sham (Figure 4C, topographical maps). We further measured the average oscillatory power of electrodes in the significant cluster. As shown in the bar plot of Figure 4C, we found the gamma power in the significant cluster was significantly increased after active-tACS ($p=.01$) and the gamma power was significantly higher in the post-active task than post-sham task ($p=.01$) (pre-sham vs. post-sham, pre-sham vs. pre-active, all $p>.05$).

For the oscillatory power in the gamma band in CTI following exogenous cue, non-parametric cluster-based permutation analysis revealed a significant increase over the frontal and central sulcus regions

(pre-active vs. post-active, p=.009), while no significant difference was observed in comparisons of neither pre-sham vs. pre-active nor pre-sham vs. post-sham (Figure 4D, topographical maps). We further measured the average oscillatory power of electrodes in the significant cluster. As shown in the bar plot of 4D, we found the gamma power in the significant cluster was significantly increased after active-tACS (p=.02) and the gamma power was significantly higher in the post-active task than post-sham task (p=.04) (pre-sham vs. post-sham, pre-sham vs. pre-active, all p>.05). Our findings revealed significant after-effects of gamma tACS on alpha band and gamma band oscillatory power. Active gamma tACS suppressed alpha power on the ipsilateral side of tACS intervention while increasing gamma power over frontal and central sulcus regions. Moreover, such modulation was consistent across endogenous and exogenous trials.

3.4 Decreasing in long-range temporal correlations following active-tACS

We applied detrended fluctuation analysis (DFA) (Peng et al. (1994)) to compute the scaling exponent α-value of EEG signal that could assess LRTC changes induced by gamma tACS. The EEG data used for DFA was the segment of CTI stages following endogenous cue or exogenous cue, the same periods as the investigation of the oscillatory power.

For the long-range temporal correlations of EEG signal in the CTI following endogenous cue, non-parametric cluster-based permutation analysis revealed a significant decrease over the right hemisphere (pre-active vs. post-active, p=.043), while no significant difference was observed in comparisons of neither pre-sham vs. pre-active nor pre-sham vs. post-sham (Figure 5A, topographical maps). We further measured the average α-value of electrodes in the significant cluster. As shown in the bar plot of 5A, we found the α-value in the significant cluster was significantly decreased after active-tACS (p=.01) and the α-value was significantly lower in the post-active task than post-sham task (p=.02) (pre-sham vs. post-sham, pre-sham vs. pre-active, all p>.05).

For the long-range temporal correlations of EEG signal in the CTI following exogenous cue, non-parametric cluster-based permutation analysis revealed a significant decrease over the right hemisphere (pre-active vs. post-active, p=.031), while no significant difference was observed in comparisons of neither pre-sham vs. pre-active nor pre-sham vs. post-sham (Figure 5B, topographical maps). We further measured the average α-value of electrodes in the significant cluster. As shown in the bar plot of Figure 5B, we found the α-value in the significant cluster was significantly decreased after active-tACS (p=.04) and the α-value was significantly lower in the post-active task than post-sham task (p=.02) (pre-sham vs. post-sham, pre-sham vs. pre-active, all p>.05). We revealed an after-effect of gamma tACS on LRTC during CTI. The α-value, which was an indicator of LRTC, was significantly decreased on the ipsilateral side of tACS intervention after active tACS, but not after sham tACS. Similar to our findings of oscillatory power, such modulation effect in CTI was consistent across endogenous and exogenous trials.

4 DISCUSSION

We showed that the after-effect of 40 Hz tACS could enhance performance in a visuo-spatial attention task, particularly by reducing reaction time. This enhancement effect happens in endogenous trials with both valid and invalid targets and exogenous trials with valid targets. Further, we analyzed the EEG signal recorded during both the pre-tACS and post-tACS task and revealed the after-effects of gamma tACS on neural activities including event-related potential, oscillatory power, and long-range temporal correlations.

4.1 Gamma tACS reduces reaction time in visuo-spatial attention task

We observed that subjects in the sham group exhibited shorter average reaction times in the post-sham task compared to the pre-sham task (Figure 2), which is significant in Endo-Valid and Exo-Valid trials while not significant in Endo-Invalid and Exo-Invalid trials. This reduction in reaction time suggests that subjects became more familiar with the task (Ghuntla et al. (2014); Clark et al. (2015)). For subjects in the active group, the reaction times were significantly reduced after active tACS intervention but such enhancement is task-specific that not all forms of attention were equally susceptible to gamma tACS (Figure 2). The reaction time of endogenous trials in visuo-spatial attention task were found to be reduced in online gamma tACS studies, but not exogenous trials (Hopfinger et al. (2017); Kasten et al. (2020)). While the current study found reductions of reaction time in endogenous trials which were consistent with previous studies, we also probed a significant reduction of reaction time in exogenous trials with valid targets but not invalid targets. Such different findings can be rooted in different mechanisms of the acute and lasting effects of oscillating electric fields (He et al. (2023)). The neuron spike timing was significantly synchronized at the stimulation frequency of online tACS by a sub-threshold resonance effect (Johnson et al. (2020); Schmidt et al. (2014)). Our findings indicate that the reduction in reaction time is not limited to the period during gamma tACS intervention, as seen in previous studies (Hopfinger et al. (2017); Kasten et al. (2020)), but also persists after the stimulation, suggesting a lasting effect of gamma tACS on visuo-spatial attention. The after-effects of offline tACS may be related to long-term potentiation (LTP) which increasing synaptic strength (Zaehle et al. (2010); Vossen et al. (2015)).

Moreover, our results demonstrate that a single stimulation protocol does not uniformly benefit all subtypes of visuo-spatial attention. Specifically, while we observed significant improvements in endogenous attention tasks, the same was not true for all exogenous attention tasks, highlighting the complexity and specificity of neural mechanisms underlying different types of attention (Wang et al. (2015); Dugué et al. (2020)). This specificity underscores the need for tailored tACS protocols to target distinct attentional processes effectively. Recent findings suggested that synaptic modulation in visual cortices can significantly impact the processing of exogenously cued stimuli; specifically, stronger activity modulation in visuo-occipital areas has been observed during tasks involving involuntary attention to external cues (Dugué et al. (2020)). The responsiveness of neurons in the primary visual cortex (V1) to exogenous cues has been shown to vary depending on the stimulus onset asynchrony and the novelty of the cue, further underscoring the role of synaptic dynamics in parieto-occipital region in mediating exogenous attention (Wang et al. (2015)). Additionally, the differential effects on valid versus invalid trials suggest that gamma tACS selectively enhance attentional processes that are more predictable or have a higher degree of expectancy.

The specificity of gamma-band intervention in enhancing task performance is likely due to the role of gamma oscillations in visuo-spatial attention. Gamma-band oscillations facilitate the synchronization of neuronal activity across different brain regions, crucial for integrating sensory information and maintaining attention (Kaiser and Lutzenberger (2003)). These oscillations are specifically linked to the processing of visual and spatial information and are involved in the top-down control of attention, allowing the brain to focus on relevant stimuli while filtering out distractions (Han et al. (2022)). Transcranial alternating current stimulation (tACS) can modulate brain activity by entraining neuronal oscillations to the frequency of the applied current. When tACS is applied at gamma frequencies, it enhances gamma-band oscillations in the brain, thereby improving cognitive functions associated with these oscillations, such as visuo-spatial attention (Tavakoli and Yun (2017); Krause et al. (2022)). This effect is due to tACS competing with ongoing neural oscillations to control the timing of neuronal spikes, which is more effective when the stimulation frequency matches the natural oscillatory frequency of the target neurons (Krause et al. (2022)).

For visuo-spatial attention, which relies heavily on gamma-band activity, tACS at gamma frequencies can effectively entrain neuronal activity, enhancing performance in tasks requiring visuo-spatial attention.

4.2 Gamma tACS modulates amplitude and latency of event-related potentials

We observed the after-effects of gamma tACS on the event-related potential, particularly the amplitude of the N1 component (Figure 3A) as well as the amplitude (Figure 3B) and latency (Figure 3C) of the P3 component. Our findings extend the modulation effects of tACS on ERP beyond the immediate period of gamma tACS intervention, as shown in previous studies (Radecke et al. (2023)), to include significant after-effects observed post-intervention. This persistent modulation underscores the potential for gamma tACS to induce lasting changes in neural processing, possibly through mechanisms such as NMDA receptor-mediated spike-timing plasticity (Zaehle et al. (2010); Wischnewski et al. (2019)).

Significant changes were found in Endo-Valid, Endo-Invalid, and Exo-Valid trials but not Exo-Invalid trials, which aligned with our findings of non-uniform reduction in reaction time (Figure 2). This specificity highlights the nuanced impact of tACS on attentional networks, which may require tailored protocols for optimal effectiveness. Furthermore, our results demonstrate that both early ERP components like N1 and later components like P3 can be affected by tACS. The N1 component was linked to the early processing of directing attention toward a specific location in the visual field (Di Russo et al. (2003)). The amplitude of P3 was indicative of the allocation of attentional resources and larger P3 amplitudes suggested greater attentional engagement in the task (Chueh et al. (2017); Chang et al. (2015)). The latency of P3 reflected the speed of cognitive processing that shorter latency was typically associated with faster response speed (Miniussi et al. (1999)). This indicates that gamma tACS can influence multiple stages of neural processing in attention tasks. As for the modulation of tACS on ERP in visuo-spatial attention tasks, a recent study found that the amplitude of visual ERP showed reduced lateralization over the posterior site induced by online alpha tACS (Radecke et al. (2023)), due to lasting change by NMDA receptor mediated spike-timing plasticity (Zaehle et al. (2010); Wischnewski et al. (2019)). The current study further provided evidence that offline gamma tACS could modulate N1 and P3 components of ERP. These findings suggest that gamma tACS has the potential for broader applications in cognitive enhancement and therapeutic interventions by modulating both early and late stages of attention-related neural activity.

4.3 Increase/decrease of oscillatory power in cue-target interval of visuo-spatial attention task due to gamma tACS

The analysis of oscillatory power in the CTI period of the visuo-spatial attention task revealed a band-specific but not task-specific change of oscillation power induced by offline gamma tACS (Figure 4). Our findings reveal that the modulation effect of tACS on oscillatory power extends beyond the immediate period of stimulation, demonstrating significant after-effects post-intervention. We noticed a post-active significant decrease in alpha band power on the ipsilateral side of tACS intervention and such after-effect was shown in both endogenous (Figure 4A) and exogenous trials (Figure 4B). As for the gamma band power, we observed a post-active significant increase over the frontal and central sulcus regions, which is also consistent across endogenous (Figure 4C) and exogenous (Figure 4D) trials. This consistency across task types suggests a robust and generalizable effect of gamma tACS on neural oscillatory dynamics. We intended to increase gamma band synchronization by using in-phase gamma tACS, and our results indicated an increase in oscillatory power in the gamma band (Figure 4 C and D). This finding demonstrates that in-phase tACS can effectively enhance synchronization in specific frequency bands. Changes in oscillatory brain activity induced by rhythmic transcranial brain stimulation can persist after the end of stimulation intervention (Veniero et al. (2015)). The after-effect of gamma tACS in 40 Hz was found to either strengthen

or weaken interhemispheric coherence in the gamma range depending on whether the bilateral stimulation on occipital regions was delivered by an in-phase or anti-phase protocol Helfrich et al. (2015); Strüber et al. (2014). Another study applied 30 Hz HD-tACS over the left auditory cortex of dyslexia patients and found a significant 30 Hz-power increase in the left auditory cortex and superior temporal gyrus but a 30 Hz-power decrease in the right superior temporal gyrus after tACS intervention Marchesotti et al. (2020).

Our results indicate that gamma tACS can modulate oscillatory power not only in the gamma band but also in other frequency bands, such as the alpha band. One possible explanation for this cross-frequency modulation is the interdependent nature of neural oscillations, where changes in one frequency band can influence the dynamics of other bands through mechanisms like cross-frequency coupling and resonance effects (Sotero (2016)). Combining our findings of behavioral performance and oscillatory power, the desynchronization of alpha-band activity in cue-target interval represented selective inhibition of irrelevant sensory information in visual space thus facilitating quicker and more engaged processing of the upcoming target, potentially leading to shorter reaction times (Foxe and Snyder (2011)). What's more, post-cue alpha gamma ratio was found to represent a significant negative correlation with response time in an attentional task, meaning higher power of gamma oscillations and lower power of alpha oscillations could lead to faster response speed (Fahimi et al. (2018)).

The observation that gamma tACS applied over the parieto-occipital region resulted in significant gamma power changes in frontal activities can be explained by several factors related to the nature of brain connectivity and the effects of tACS. Firstly, gamma oscillations play a crucial role in various cognitive processes involving multiple brain regions working in concert. The frontoparietal network, for instance, is heavily involved in cognitive control and working memory, and gamma-band activity in this network can be modulated by stimulation in either the frontal or parietal regions (Kvašňák et al. (2023); Wang et al. (2023); Brown et al. (2024)). This feature of interconnection suggests that gamma tACS applied to the parietal and occipital regions can propagate its effects to the frontal cortex through these networks. Additionally, tACS is a non-invasive method that delivers alternating current through the scalp, with electrical fields that can spread beyond the targeted areas, leading to off-target effects in regions such as the frontal cortex (Mencarelli et al. (2022)). This is supported by biophysical modeling studies showing that tACS can affect both local and distant brain areas. Furthermore, gamma-band synchronization between different brain regions is well-documented, facilitating communication and integration of information (Iwaki (2013); Brown et al. (2024)). Thus, tACS applied to the parietal and occipital regions can enhance gamma synchronization, reflected in increased gamma power in the frontal regions due to their functional connectivity. Lastly, the specific cognitive tasks or states during which EEG measurements are taken can influence gamma power changes. Tasks requiring significant cognitive control or working memory might naturally involve increased gamma activity in the frontal cortex, which could be further modulated by tACS applied to connected regions (Rochart et al. (2020); Kvašňák et al. (2023)).

In summary, the current study revealed the decrease in alpha power combined with the increase in gamma power after active gamma tACS suggests that gamma tACS enhances the selective processing of relevant stimuli while suppressing irrelevant information. This dual modulation likely contributes to the observed enhancement in attentional performance.

4.4 Decrease of long-range temporal correlations due to gamma tACS

Besides the investigation of oscillatory power in the CTI period, we also analyzed the long-range temporal correlations (LRTC) of EEG signal during CTI (Figure 5) which represented the after-effect of gamma tACS on the temporal complexity of EEG signal. The indicator of LRTC was the α-value obtained by

detrended fluctuation analysis (DFA). We found a significant decrease of α-value on the ipsilateral side of tACS intervention and such after-effect of active tACS was consistent across endogenous (Figure 5A) and exogenous trials (Figure 5A). This change in LRTC, indexed by the α-value, aligns with our oscillatory power findings to some extent. Specifically, an α-value of 0.5 corresponds to white noise, 1 to pink noise, and 1.5 to Brownian noise, with the slope of the power spectrum steepening as the α-value increases (Peng et al. (1994); Gebber et al. (2006)). Therefore, the observed decrease in alpha band power and increase in gamma band power could result in a flatter power spectrum slope, which is consistent with a reduction in the α-value. This alignment underscores the interconnected nature of neural oscillations and temporal complexity, where modulating one aspect of neural activity can influence others. Combining our findings of reaction time and LRTC, we observed subjects in the active group achieved reductions of reaction times (except for Exo-Invalid trials) as well as a decrease of LRTC on the right hemisphere, which was aligned with a previous study that fast reaction time was associated with low LRTC during the task (Irrmischer et al. (2018)). These results highlight the potential of gamma tACS to enhance cognitive performance by modulating both the spectral and temporal dynamics of neural activity.

4.5 Implications for Clinical and Cognitive Enhancement

Our findings have implications for both clinical applications and cognitive enhancement. In the current study, we observed that gamma tACS not only reduced reaction times during the intervention but also had lasting effects post-intervention, highlighting its potential to induce long-term potentiation (LTP) in neural circuits. This suggests that gamma tACS could be a valuable tool for enhancing visuo-spatial attention over extended periods. For instance, in the treatment of Attention Deficit Hyperactivity Disorder (ADHD), which is characterized by hyperactivity, impulsivity, and inattention, tACS has shown promise (Boetzel and Herrmann (2021); Farokhzadi et al. (2021); Amouzadeh and Sheikh (2022)). Studies have demonstrated that tACS can improve working memory and selective attention in ADHD patients, offering an alternative to traditional pharmacological treatments that can have significant side effects. Specifically, tACS protocols have been found to be more effective and durable compared to medications like Ritalin in reducing ADHD symptoms. Beyond clinical applications, our results also suggest that tACS can enhance cognitive functions in healthy individuals (Reteig et al. (2017)). For example, it has been used to improve visual attention and performance in tasks requiring high levels of concentration, such as eSports (Jiao et al. (2024)). This indicates that tACS could be utilized to boost cognitive performance in various domains, making it a versatile tool for both therapeutic and enhancement purposes.

In conclusion, the current study revealed the after-effect of gamma tACS towards the right parieto-occipital region on behavioral performance and neural activity in a visuo-spatial attention task. In a single-blind, sham-controlled, and between-group experiment design, 20 young and healthy subjects were assigned to two groups receiving either sham tACS or active tACS at 40 Hz. Subjects performed a version of the Posner cueing task with EEG recording once before and once after the tACS intervention. We found the reaction time of subjects in the active group was significantly reduced after tACS intervention, and significantly faster than subjects in the sham group after sham-tACS. Such significant reductions of reaction time were not uniformly observed in all trial types. Further, the analysis of EEG signal revealed the after-effects of gamma tACS on event-related potential, oscillatory power, and long-range temporal correlations. The amplitude of the N1 component as well as the amplitude and latency of the P3 component were changed due to active gamma tACS, and such modulation was specific in trial types. The oscillatory power during cue-target interval showed consistent change in trial types but varied in frequency band due to gamma tACS: decrease in alpha band power but increase in gamma band power. Lastly, detrended fluctuation analysis of EEG signal during cue-target interval showed decrease of long-range temporal

correlations on the ipsilateral side after gamma tACS. This study provided evidence that offline gamma tACS can modulate reaction time and electrophysiological activity in the visuo-spatial attention task. Implications based on current results can help understand the after-effects of tACS and develop more effective non-invasive stimulation protocols to enhance cognitive performance in clinical and healthy populations.

ETHICS STATEMENT

This study was approved by the Research Ethics Committee at The University of Tokyo based on the Research Ethics Review Implementation Rules of The University of Tokyo (21-271, 22-432). The main trial was conducted according to the guidelines of the Declaration of Helsinki. The participants provided their written informed consent to participate in this study.

CONFLICT OF INTEREST STATEMENT

The authors declare no competing interest.

AUTHOR CONTRIBUTIONS

TZ: Conceptualization, Methodology, Software, Validation, Formal analysis, Investigation, Data Curation, Writing - Original Draft, Writing - Review & Editing, Visualization, Project administration, Funding acquisition. YH: Formal analysis, Writing - Original Draft, Visualization. MS: Methodology, Software, Investigation, Resources, Writing - Original Draft. KS: Writing - Review & Editing, Supervision, Project administration, Funding acquisition. YJ: Resources, Writing - Review & Editing, Project administration, Funding acquisition. KK: Conceptualization, Resources, Writing - Review & Editing, Supervision, Project administration, Funding acquisition.

FUNDING

This research is partially supported by Japan Society for the Promotion of Science through a Grant-in-Aid for DC1 Fellows (KAKENHI), Grant No. 22J22909, to T.Z., Japan Society for the Promotion of Science through Grants-in-Aid for Scientific Research (KAKENHI), Grant No. 22K19785, Asahi Glass Foundation, and The Precise Measurement Technology Promotion Foundation to K.K..

DATA AVAILABILITY STATEMENT

The data has not been shared in a public repository due to the privacy rights of human subjects. However, the data and analysis tools used in the current study are available from the corresponding author upon reasonable request.

REFERENCES

(2018). ROAST: an open-source, fully-automated, Realistic vOlumetric-Approach-based Simulator for TES (Honolulu, HI)

Abellaneda-Pérez, K., Vaqué-Alcázar, L., Perellón-Alfonso, R., Bargalló, N., Kuo, M.-F., Pascual-Leone, A., et al. (2020). Differential tdcs and tacs effects on working memory-related neural activity and resting-state connectivity. Frontiers in Neuroscience 13. doi:10.3389/fnins.2019.01440

Ablin, P., Cardoso, J.-F., and Gramfort, A. (2018). Faster independent component analysis by preconditioning with hessian approximations. IEEE Transactions on Signal Processing 66, 4040–4049. doi:10.1109/TSP.2018.2844203

Amouzadeh, F. and Sheikh, M. (2022). Impact of transcranial alternating current stimulation on working memory and selective attention in athletes with attention deficit hyperactivity disorder: randomized controlled trial. Neuroreport 33, 756—762. doi:10.1097/wnr.0000000000001842

Antal, A., Alekseichuk, I., Bikson, M., Brockmöller, J., Brunoni, A., Chen, R., et al. (2017). Low intensity transcranial electric stimulation: Safety, ethical, legal regulatory and application guidelines. Clinical Neurophysiology 128, 1774–1809. doi:https://doi.org/10.1016/j.clinph.2017.06.001

Armstrong, R. A. (2014). When to use the bonferroni correction. Ophthalmic and Physiological Optics 34, 502–508. doi:https://doi.org/10.1111/opo.12131

Babadi, B. and Brown, E. N. (2014). A review of multitaper spectral analysis. IEEE Transactions on Biomedical Engineering 61, 1555–1564. doi:10.1109/TBME.2014.2311996

Benjamini, Y. and Hochberg, Y. (1995). Controlling the false discovery rate: A practical and powerful approach to multiple testing. Journal of the Royal Statistical Society: Series B (Methodological) 57, 289–300. doi:https://doi.org/10.1111/j.2517-6161.1995.tb02031.x

Bisley, J. W. and Goldberg, M. E. (2010). Attention, intention, and priority in the parietal lobe. Annual Review of Neuroscience 33, 1–21. PMID: 20192813

Boetzel, C. and Herrmann, C. S. (2021). Chapter 6 - potential targets for the treatment of adhd using transcranial electrical current stimulation. In Non-invasive Brain Stimulation (NIBS) in Neurodevelopmental Disorders, eds. R. C. Kadosh, T. Zaehle, and K. Krauel (Elsevier), vol. 264 of Progress in Brain Research. 151–170

Boetzel, C., Stecher, H. I., and Herrmann, C. S. (2023). Erp-aligned delta transcranial alternating current stimulation modulates the p3 amplitude. International Journal of Psychophysiology 193, 112247

Bosman, C. A., Schoffelen, J.-M., Brunet, N., Oostenveld, R., Bastos, A. M., Womelsdorf, T., et al. (2012). Attentional stimulus selection through selective synchronization between monkey visual areas. Neuron 75, 875–888. doi:https://doi.org/10.1016/j.neuron.2012.06.037

Braga, M., Barbiani, D., Emadi Andani, M., Villa-Sánchez, B., Tinazzi, M., and Fiorio, M. (2021). The role of expectation and beliefs on the effects of non-invasive brain stimulation. Brain Sciences 11

Brown, T., Kim, K., Gehring, W. J., Lustig, C., and Bohnen, N. I. (2024). Sensitivity to and control of distraction: Distractor-entrained oscillation and frontoparietal eeg gamma synchronization. Brain Sciences 14. doi:10.3390/brainsci14060609

Chang, Y.-K., Pesce, C., Chiang, Y.-T., Kuo, C.-Y., and Fong, D.-Y. (2015). Antecedent acute cycling exercise affects attention control: an erp study using attention network test. Frontiers in Human Neuroscience 9, 156. doi:10.3389/fnhum.2015.00156

Chen, X., Shi, X., Wu, Y., Zhou, Z., Chen, S., Han, Y., et al. (2022). Gamma oscillations and application of 40-hz audiovisual stimulation to improve brain function. Brain and Behavior 12, e2811. doi:https://doi.org/10.1002/brb3.2811

Chueh, T.-Y., Huang, C.-J., Hsieh, S.-S., Chen, K.-F., Chang, Y.-K., and Hung, T.-M. (2017). Sports training enhances visuo-spatial cognition regardless of open-closed typology. PeerJ 5, e3336. doi:10.7717/peerj.3336

Clark, K., Appelbaum, L. G., van den Berg, B., Mitroff, S. R., and Woldorff, M. G. (2015). Improvement in visual search with practice: Mapping learning-related changes in neurocognitive stages of processing. Journal of Neuroscience 35, 5351–5359. doi:10.1523/JNEUROSCI.1152-14.2015

Corbetta, M. and Shulman, G. L. (2002). Control of goal-directed and stimulus-driven attention in the brain. Nature Reviews Neuroscience 3, 201–215. doi:10.1038/nrn755

Davis, M.-C., Fitzgerald, P. B., Bailey, N. W., Sullivan, C., Stout, J. C., Hill, A. T., et al. (2023). Effects of medial prefrontal transcranial alternating current stimulation on neural activity and connectivity in people with huntington's disease and neurotypical controls. Brain Research 1811, 148379. doi:https://doi.org/10.1016/j.brainres.2023.148379

Di Russo, F., Martínez, A., and Hillyard, S. A. (2003). Source Analysis of Event-related Cortical Activity during Visuo-spatial Attention. Cerebral Cortex 13, 486–499. doi:10.1093/cercor/13.5.486

[Dataset] Documentation, S. (2020). Simulation and model-based design

Du, X. D., Li, Z., Yuan, N., Yin, M., Zhao, X. L., Lv, X. L., et al. (2022). Delayed improvements in visual memory task performance among chronic schizophrenia patients after high-frequency repetitive transcranial magnetic stimulation. World J Psychiatry 12, 1169–1182. doi:10.5498/wjp.v12.i9.1169

Dugué, L., Merriam, E. P., Heeger, D. J., and Carrasco, M. (2017). Specific Visual Subregions of TPJ Mediate Reorienting of Spatial Attention. Cerebral Cortex 28, 2375–2390. doi:10.1093/cercor/bhx140

Dugué, L., Merriam, E. P., Heeger, D. J., and Carrasco, M. (2020). Differential impact of endogenous and exogenous attention on activity in human visual cortex. Scientific Reports 10, 21274. doi:10.1038/s41598-020-78172-x

Eimer, M. (1999). Attending to quadrants and ring-shaped regions: Erp effects of visual attention in different spatial selection tasks. Psychophysiology 36, 491–503. doi:https://doi.org/10.1017/S0048577299980915

Elyamany, O., Leicht, G., Herrmann, C. S., and Mulert, C. (2021). Transcranial alternating current stimulation (tacs): from basic mechanisms towards first applications in psychiatry. European Archives of Psychiatry and Clinical Neuroscience 271, 135–156

Fahimi, F., Goh, W. B., Lee, T.-S., and Guan, C. (2018). Neural indexes of attention extracted from eeg correlate with elderly reaction time in response to an attentional task. In Proceedings of the 3rd International Conference on Crowd Science and Engineering (New York, NY, USA: Association for Computing Machinery), ICCSE'18. doi:10.1145/3265689.3265722

Farokhzadi, F., Mohamadi, M. R., Khajevand Khosli, A., Akbarfahimi, M., Ali Beigi, N., and Torabi, P. (2021). Comparing the effectiveness of the transcranial alternating current stimulation (tacs) and ritalin on symptoms of attention deficit hyperactivity disorder in 7-14-year-old children. Acta Medica Iranica 58, 637–648. doi:10.18502/acta.v58i12.5156

Fingelkurts, A. A. and Fingelkurts, A. A. (2014). Eeg oscillatory states: Universality, uniqueness and specificity across healthy-normal, altered and pathological brain conditions. PLOS ONE 9, 1–20. doi:10.1371/journal.pone.0087507

Foxe, J. J. and Snyder, A. C. (2011). The role of alpha-band brain oscillations as a sensory suppression mechanism during selective attention. Frontiers in Psychology 2. doi:10.3389/fpsyg.2011.00154

Fröhlich, F. (2014). Endogenous and exogenous electric fields as modifiers of brain activity: rational design of noninvasive brain stimulation with transcranial alternating current stimulation. Dialogues Clin Neurosci. 16, 93–102

Gebber, G. L., Orer, H. S., and Barman, S. M. (2006). Fractal noises and motions in time series of presympathetic and sympathetic neural activities. Journal of Neurophysiology 95, 1176–1184. doi:10.1152/jn.01021.2005. PMID: 16306172

Ghuntla, T. P., Mehta, H. B., Gokhale, P. A., and Shah, C. J. (2014). Influence of practice on visual reaction time. Journal of Mahatma Gandhi Institute of Medical Sciences 19, 119 – 122

Giustiniani, A., Tarantino, V., Bonaventura, R., Smirni, D., Turriziani, P., and Oliveri, M. (2019). Effects of low-gamma tacs on primary motor cortex in implicit motor learning. Behavioural Brain Research 376, 112170. doi:https://doi.org/10.1016/j.bbr.2019.112170

Gramfort, A., Luessi, M., Larson, E., Engemann, D. A., Strohmeier, D., Brodbeck, C., et al. (2013). MEG and EEG data analysis with MNE-Python. Frontiers in Neuroscience 7, 1–13. doi:10.3389/fnins.2013.00267

Gruber, T., Müller, M. M., Keil, A., and Elbert, T. (1999). Selective visual-spatial attention alters induced gamma band responses in the human eeg. Clinical Neurophysiology 110, 2074–2085. doi:https://doi.org/10.1016/S1388-2457(99)00176-5

Han, C., Shapley, R., and Xing, D. (2022). Gamma rhythms in the visual cortex: functions and mechanisms. Cognitive Neurodynamics 16, 745–756

Harris, C. R., Millman, K. J., van der Walt, S. J., Gommers, R., Virtanen, P., Cournapeau, D., et al. (2020). Array programming with NumPy. Nature 585, 357–362. doi:10.1038/s41586-020-2649-2

He, Y., Liu, S., Chen, L., Ke, Y., and Ming, D. (2023). Neurophysiological mechanisms of transcranial alternating current stimulation. Frontiers in Neuroscience 17, 1091925

Helfrich, R. F., Knepper, H., Nolte, G., Strüber, D., Rach, S., Herrmann, C. S., et al. (2015). Selective modulation of interhemispheric functional connectivity by hd-tacs shapes perception. PLOS Biology 12, 1–15. doi:10.1371/journal.pbio.1002031

Herwig, U., Satrapi, P., and Schönfeldt-Lecuona, C. (2003). Using the international 10-20 eeg system for positioning of transcranial magnetic stimulation. Brain Topography 16, 95–99. doi:10.1023/B:BRAT.0000006333.93597.9d

Hillyard, S. A. and Anllo-Vento, L. (1998). Event-related brain potentials in the study of visual selective attention. Proceedings of the National Academy of Sciences 95, 781–787. doi:10.1073/pnas.95.3.781

Homan, R. W., Herman, J., and Purdy, P. (1987). Cerebral location of international 10–20 system electrode placement. Electroencephalography and Clinical Neurophysiology 66, 376–382

Hopfinger, J. B., Parsons, J., and Fröhlich, F. (2017). Differential effects of 10-hz and 40-hz transcranial alternating current stimulation (tacs) on endogenous versus exogenous attention. Cogn Neurosci 8, 102–111

Hoy, K. E., Bailey, N., Arnold, S., Windsor, K., John, J., Daskalakis, Z. J., et al. (2015). The effect of γ-tacs on working memory performance in healthy controls. Brain and Cognition 101, 51–56. doi:https://doi.org/10.1016/j.bandc.2015.11.002

Huang, Y., Datta, A., Bikson, M., and Parra, L. (2019). Realistic volumetric-approach to simulate transcranial electric stimulation – roast – a fully automated open-source pipeline. Journal of Neural Engineering 16

Huang, Y., Parra, L., and Haufe, S. (2016). The new york head - a precise standardized volume conductor model for eeg source localization and tes targeting. NeuroImage 140, 150–162

Imbert, L., Moirand, R., Bediou, B., Koenig, O., Chesnoy, G., Fakra, E., et al. (2022). A single session of bifrontal tdcs can improve facial emotion recognition in major depressive disorder: An exploratory pilot study. Biomedicines 10. doi:10.3390/biomedicines10102397

Irrmischer, M., Poil, S.-S., Mansvelder, H. D., Intra, F. S., and Linkenkaer-Hansen, K. (2018). Strong long-range temporal correlations of beta/gamma oscillations are associated with poor sustained visual attention performance. European Journal of Neuroscience 48, 2674–2683

Iwaki, S. (2013). Induced gamma-band brain responses to direct eye contact in the frontal and parietal cortices. Annual International Conference of the IEEE Engineering in Medicine and Biology Society 2013, 6183–6186. doi:10.1109/EMBC.2013.6610965

Jia, X., Smith, M. A., and Kohn, A. (2011). Stimulus selectivity and spatial coherence of gamma components of the local field potential. Journal of Neuroscience 31, 9390–9403. doi:10.1523/JNEUROSCI.0645-11.2011

Jiao, F., Zhuang, J., Nitsche, M. A., Lin, Z., Ma, Y., and Liu, Y. (2024). Application of transcranial alternating current stimulation to improve esports-related cognitive performance. Frontiers in Neuroscience 18. doi:10.3389/fnins.2024.1308370

Johnson, L., Alekseichuk, I., Krieg, J., Doyle, A., Yu, Y., Vitek, J., et al. (2020). Dose-dependent effects of transcranial alternating current stimulation on spike timing in awake nonhuman primates. Science Advances 6, eaaz2747. doi:10.1126/sciadv.aaz2747

Kaiser, J. and Lutzenberger, W. (2003). Induced gamma-band activity and human brain function. The Neuroscientist 9, 475–484. doi:10.1177/1073858403259137. PMID: 14678580

Kasten, F. H., Dowsett, J., and Herrmann, C. S. (2016). Sustained aftereffect of α-tacs lasts up to 70 min after stimulation. Frontiers in Human Neuroscience 10, 245. doi:10.3389/fnhum.2016.00245

Kasten, F. H., Wendeln, T., Stecher, H. I., and Herrmann, C. S. (2020). Hemisphere-specific, differential effects of lateralized, occipital–parietal α- versus γ-tacs on endogenous but not exogenous visual-spatial attention. Scientific Reports 10, 12270. doi:10.1038/s41598-020-68992-2

Kemmerer, S. K., de Graaf, T. A., ten Oever, S., Erkens, M., De Weerd, P., and Sack, A. T. (2022). Parietal but not temporoparietal alpha-tacs modulates endogenous visuospatial attention. Cortex 154, 149–166. doi:https://doi.org/10.1016/j.cortex.2022.01.021

Klimesch, W. (2012). Alpha-band oscillations, attention, and controlled access to stored information. Trends in Cognitive Sciences 16, 606–617

Krause, M. R., Vieira, P. G., Thivierge, J.-P., and Pack, C. C. (2022). Brain stimulation competes with ongoing oscillations for control of spike timing in the primate brain. PLOS Biology 20, 1–27. doi:10.1371/journal.pbio.3001650

Kreegipuu, K. and Allik, J. (2007). Detection of motion onset and offset: reaction time and visual evoked potential analysis. Psychological Research 71, 703–708

Krieger, D. and Dillbeck, M. (1987). High frequency scalp potentials evoked by a reaction time task. Electroencephalography and Clinical Neurophysiology 67, 222–230

Kvašňák, E., Magyarová, E., Domankuš, M., Tesař, M., Kymplová, J., Fetissov, V., et al. (2023). 10 minutes frontal 40 hz tacs—effects on working memory tested by luck-vogel task. Behavioral Sciences 13. doi:10.3390/bs13010039

Liu, S., He, Y., Guo, D., Liu, X., Hao, X., Hu, P., et al. (2023). Transcranial alternating current stimulation ameliorates emotional attention through neural oscillations modulation. Cognitive Neurodynamics 17, 1473–1483

Lorist, M. and Snel, J. (1998). Nicotine, Caffeine and Social Drinking: Behaviour and Brain Function (Routledge), 1st edn. doi:10.4324/9781315079189

Magazzini, L. and Singh, K. D. (2018). Spatial attention modulates visual gamma oscillations across the human ventral stream. NeuroImage 166, 219–229. doi:https://doi.org/10.1016/j.neuroimage.2017.10.069

Marchesotti, S., Nicolle, J., Merlet, I., Arnal, L. H., Donoghue, J. P., and Giraud, A.-L. (2020). Selective enhancement of low-gamma activity by tacs improves phonemic processing and reading accuracy in dyslexia. PLOS Biology 18, 1–23. doi:10.1371/journal.pbio.3000833

Mashal, N. and Metzuyanim-Gorelick, S. (2019). New information on the effects of transcranial direct current stimulation on n-back task performance. Experimental Brain Research 237, 1315–1324. doi:10.1007/s00221-019-05500-7

McDermott, B., Porter, E., Hughes, D., McGinley, B., Lang, M., O'Halloran, M., et al. (2018). Gamma band neural stimulation in humans and the promise of a new modality to prevent and treat alzheimer's disease. Journal of Alzheimer's Disease 65, 363–392. doi:10.3233/JAD-180391

McKinney, W. et al. (2010). Data structures for statistical computing in python. In Proceedings of the 9th Python in Science Conference (Austin, TX), vol. 445, 51–56

Meisel, C., Bailey, K., Achermann, P., and Plenz, D. (2017). Decline of long-range temporal correlations in the human brain during sustained wakefulness. Scientific Reports 7, 11825. doi:10.1038/s41598-017-12140-w

Mencarelli, L., Monti, L., Romanella, S., Neri, F., Koch, G., Salvador, R., et al. (2022). Local and distributed fmri changes induced by 40 hz gamma tacs of the bilateral dorsolateral prefrontal cortex: A pilot study. Neural Plasticity 2022, 6197505. doi:https://doi.org/10.1155/2022/6197505

Miniussi, C., Wilding, E. L., Coull, J. T., and Nobre, A. C. (1999). Orienting attention in time: Modulation of brain potentials. Brain 122, 1507–1518. doi:10.1093/brain/122.8.1507

Morales, S. and Bowers, M. E. (2022). Time-frequency analysis methods and their application in developmental eeg data. Developmental Cognitive Neuroscience 54, 101067. doi:https://doi.org/10.1016/j.dcn.2022.101067

Murphy, O., Hoy, K., Wong, D., Bailey, N., Fitzgerald, P., and Segrave, R. (2020). Transcranial random noise stimulation is more effective than transcranial direct current stimulation for enhancing working memory in healthy individuals: Behavioural and electrophysiological evidence. Brain Stimulation 13, 1370–1380. doi:https://doi.org/10.1016/j.brs.2020.07.001

Nakao, T., Miyagi, M., Hiramoto, R., Wolff, A., Gomez-Pilar, J., Miyatani, M., et al. (2019). From neuronal to psychological noise – long-range temporal correlations in eeg intrinsic activity reduce noise in internally-guided decision making. NeuroImage 201, 116015. doi:https://doi.org/10.1016/j.neuroimage.2019.116015

Nakazono, H., Ogata, K., Takeda, A., Yamada, E., Kimura, T., and Tobimatsu, S. (2020). Transcranial alternating current stimulation of α but not β frequency sharpens multiple visual functions. Brain Stimulation 13, 343–352

Nomura, T., Asao, A., and Kumasaka, A. (2019). Transcranial alternating current stimulation over the prefrontal cortex enhances episodic memory recognition. Experimental Brain Research 237, 1709–1715. doi:10.1007/s00221-019-05543-w

Osaki, S., Amimoto, K., Miyazaki, Y., Tanabe, J., and Yoshihiro, N. (2021). Investigating the characteristics of covert unilateral spatial neglect using the modified posner task: A single-subject design study. Progress in Rehabilitation Medicine 6

Palva, J. M., Zhigalov, A., Hirvonen, J., Korhonen, O., Linkenkaer-Hansen, K., and Palva, S. (2013). Neuronal long-range temporal correlations and avalanche dynamics are correlated with behavioral scaling laws. Proceedings of the National Academy of Sciences 110, 3585–3590. doi:10.1073/pnas.1216855110

Park, S., Choi, D., Yi, J., Lee, S., Lee, J. E., Choi, B., et al. (2017). Effects of display curvature, display zone, and task duration on legibility and visual fatigue during visual search task. Applied Ergonomics 60, 183–193

Peng, C.-K., Buldyrev, S. V., Havlin, S., Simons, M., Stanley, H. E., and Goldberger, A. L. (1994). Mosaic organization of dna nucleotides. Phys Rev E Stat Phys Plasmas Fluids Relat Interdiscip Topics 49, 1685–1689

Posner, M. I., Snyder, C. R., and Davidson, B. J. (1980). Attention and the detection of signals. Journal of Experimental Psychology: General 109, 160–174

Radecke, J.-O., Fiene, M., Misselhorn, J., Herrmann, C. S., Engel, A. K., Wolters, C. H., et al. (2023). Personalized alpha-tacs targeting left posterior parietal cortex modulates visuo-spatial attention and posterior evoked eeg activity. Brain Stimulation 16, 1047–1061. doi:https://doi.org/10.1016/j.brs.2023.06.013

Reteig, L. C., Talsma, L. J., van Schouwenburg, M. R., and Slagter, H. A. (2017). Transcranial electrical stimulation as a tool to enhance attention. Journal of Cognitive Enhancement 1, 10–25

Riddle, J., Hwang, K., Cellier, D., Dhanani, S., and D'Esposito, M. (2019). Causal Evidence for the Role of Neuronal Oscillations in Top–Down and Bottom–Up Attention. Journal of Cognitive Neuroscience 31, 768–779

Rochart, R., Liu, Q., Fonteh, A. N., Harrington, M. G., and Arakaki, X. (2020). Compromised behavior and gamma power during working memory in cognitively healthy individuals with abnormal csf amyloid/tau. Frontiers in Aging Neuroscience 12. doi:10.3389/fnagi.2020.574214

Romanella, S., Mencarelli, L., Burke, M., et al. (2023). Targeting neural correlates of placebo effects. Cognitive, Affective, & Behavioral Neuroscience 23, 217–236

Sadeghi, N. and Nazari, M. A. (2015). Effect of neurofeedback on visual-spatial attention in male children with reading disabilities: An event-related potential study. Neuroscience and Medicine 6, 71–79. doi:10.4236/nm.2015.62013

SAITO, H., KANAYAMA, S., and TAKAHASHI, T. (1992). Right angular lesion and selective impairment of motion vision in left visual field. The Tohoku Journal of Experimental Medicine 166, 229–238. doi:10.1620/tjem.166.229

Schmidt, S. L., Iyengar, A. K., Foulser, A. A., Boyle, M. R., and Fröhlich, F. (2014). Endogenous cortical oscillations constrain neuromodulation by weak electric fields. Brain Stimulation 7, 878–889

Schuhmann, T., Kemmerer, S. K., Duecker, F., de Graaf, T. A., ten Oever, S., De Weerd, P., et al. (2019). Left parietal tacs at alpha frequency induces a shift of visuospatial attention. PLOS ONE 14, 1–25. doi:10.1371/journal.pone.0217729

Seabold, S. and Perktold, J. (2010). statsmodels: Econometric and statistical modeling with python. In 9th Python in Science Conference

Shapiro, S. S. and Wilk, M. B. (1965). An analysis of variance test for normality (complete samples). Biometrika 52, 591–611

Slepian, D. (1978). Prolate spheroidal wave functions, fourier analysis, and uncertainty — v: the discrete case. The Bell System Technical Journal 57, 1371–1430. doi:10.1002/j.1538-7305.1978.tb02104.x

Somers, D. C. and Sheremata, S. L. (2013). Attention maps in the brain. WIREs Cognitive Science 4, 327–340

Sotero, R. C. (2016). Topology, cross-frequency, and same-frequency band interactions shape the generation of phase-amplitude coupling in a neural mass model of a cortical column. PLOS Computational Biology 12, 1–29. doi:10.1371/journal.pcbi.1005180

Spooner, R. K., Wiesman, A. I., Proskovec, A. L., Heinrichs-Graham, E., and Wilson, T. W. (2020). Prefrontal theta modulates sensorimotor gamma networks during the reorienting of attention. Human Brain Mapping 41, 520–529. doi:https://doi.org/10.1002/hbm.24819

[Dataset] stfbnc and Katz, D. S. (2023). stfbnc/fathon: v1.3.3. doi:10.5281/zenodo.10155742

Strüber, D., Rach, S., Trautmann-Lengsfeld, S. A., Engel, A. K., and Herrmann, C. S. (2014). Antiphasic 40 hz oscillatory current stimulation affects bistable motion perception. Brain Topography 27, 158–171. doi:10.1007/s10548-013-0294-x

Studer, B., Cen, D., and Walsh, V. (2014). The angular gyrus and visuospatial attention in decision-making under risk. NeuroImage 103, 75–80. doi:https://doi.org/10.1016/j.neuroimage.2014.09.003

Sugimura, K., Iwasa, Y., Kobayashi, R., Honda, T., Hashimoto, J., Kashihara, S., et al. (2021). Association between long-range temporal correlations in intrinsic eeg activity and subjective sense of identity. Scientific Reports 11, 422. doi:10.1038/s41598-020-79444-2

Sur, S. and Sinha, V. K. (2009). Event-related potential: An overview. Industrial Psychiatry Journal 18

Szewczyk, M., Augustynowicz, P., and Szubielska, M. (2022). Implicit spatial sequential learning facilitates attentional selection in covert visual search. an event-related potentials study. Frontiers in Human Neuroscience 16. doi:10.3389/fnhum.2022.974791

Tavakoli, A. V. and Yun, K. (2017). Transcranial alternating current stimulation (tacs) mechanisms and protocols. Frontiers in Cellular Neuroscience 11. doi:10.3389/fncel.2017.00214

ten Oever, S., de Graaf, T. A., Bonnemayer, C., Ronner, J., Sack, A. T., and Riecke, L. (2016). Stimulus presentation at specific neuronal oscillatory phases experimentally controlled with tacs: Implementation and applications. Frontiers in Cellular Neuroscience 10. doi:10.3389/fncel.2016.00240

Tendolkar, I., Ruhrmann, S., Brockhaus-Dumke, A., Pauli, M., Mueller, R., Pukrop, R., et al. (2005). Neural correlates of visuo-spatial attention during an antisaccade task in schizophrenia: an erp study. The International journal of neuroscience 115, 681–698. doi:10.1080/00207450590887475

Thut, G., Nietzel, A., Brandt, S. A., and Pascual-Leone, A. (2006). α-band electroencephalographic activity over occipital cortex indexes visuospatial attention bias and predicts visual target detection. Journal of Neuroscience 26, 9494–9502. doi:10.1523/JNEUROSCI.0875-06.2006

Veniero, D., Vossen, A., Gross, J., and Thut, G. (2015). Lasting eeg/meg aftereffects of rhythmic transcranial brain stimulation: Level of control over oscillatory network activity. Frontiers in Cellular Neuroscience 9. doi:10.3389/fncel.2015.00477

Vergara, V. M., Weiland, B. J., Hutchison, K. E., and Calhoun, V. D. (2018). The impact of combinations of alcohol, nicotine, and cannabis on dynamic brain connectivity. Neuropsychopharmacology 43, 877–890. doi:10.1038/npp.2017.280

Virtanen, P., Gommers, R., Oliphant, T. E., Haberland, M., Reddy, T., Cournapeau, D., et al. (2020). SciPy 1.0: Fundamental Algorithms for Scientific Computing in Python. Nature Methods 17, 261–272. doi:10.1038/s41592-019-0686-2

Vossen, A., Gross, J., and Thut, G. (2015). Alpha power increase after transcranial alternating current stimulation at alpha frequency (α-tacs) reflects plastic changes rather than entrainment. Brain Stimulation 8, 499–508. doi:https://doi.org/10.1016/j.brs.2014.12.004

Wang, F., Chen, M., Yan, Y., Zhaoping, L., and Li, W. (2015). Modulation of neuronal responses by exogenous attention in macaque primary visual cortex. Journal of Neuroscience 35, 13419–13429. doi:10.1523/JNEUROSCI.0527-15.2015

Wang, X., Jian, O., Kang, A., Wang, L., Zhang, J., Yan, T., et al. (2023). Gamma tacs reshapes low-dimensional trajectories of brain activity in working memory. 2023 17th International Conference on Complex Medical Engineering (CME) , 98–102

Wischnewski, M., Engelhardt, M., Salehinejad, M. A., Schutter, D. J. L. G., Kuo, M. F., and Nitsche, M. A. (2019). NMDA Receptor-Mediated Motor Cortex Plasticity After 20 Hz Transcranial Alternating Current Stimulation. Cerebral Cortex 29, 2924–2931. doi:10.1093/cercor/bhy160

Zaehle, T., Rach, S., and Herrmann, C. S. (2010). Transcranial alternating current stimulation enhances individual alpha activity in human eeg. PLOS ONE 5, 1–7

Zani, A., Tumminelli, C., and Proverbio, A. M. (2020). Electroencephalogram (eeg) alpha power as a marker of visuospatial attention orienting and suppression in normoxia and hypoxia. an exploratory study. Brain Sciences 10. doi:10.3390/brainsci10030140

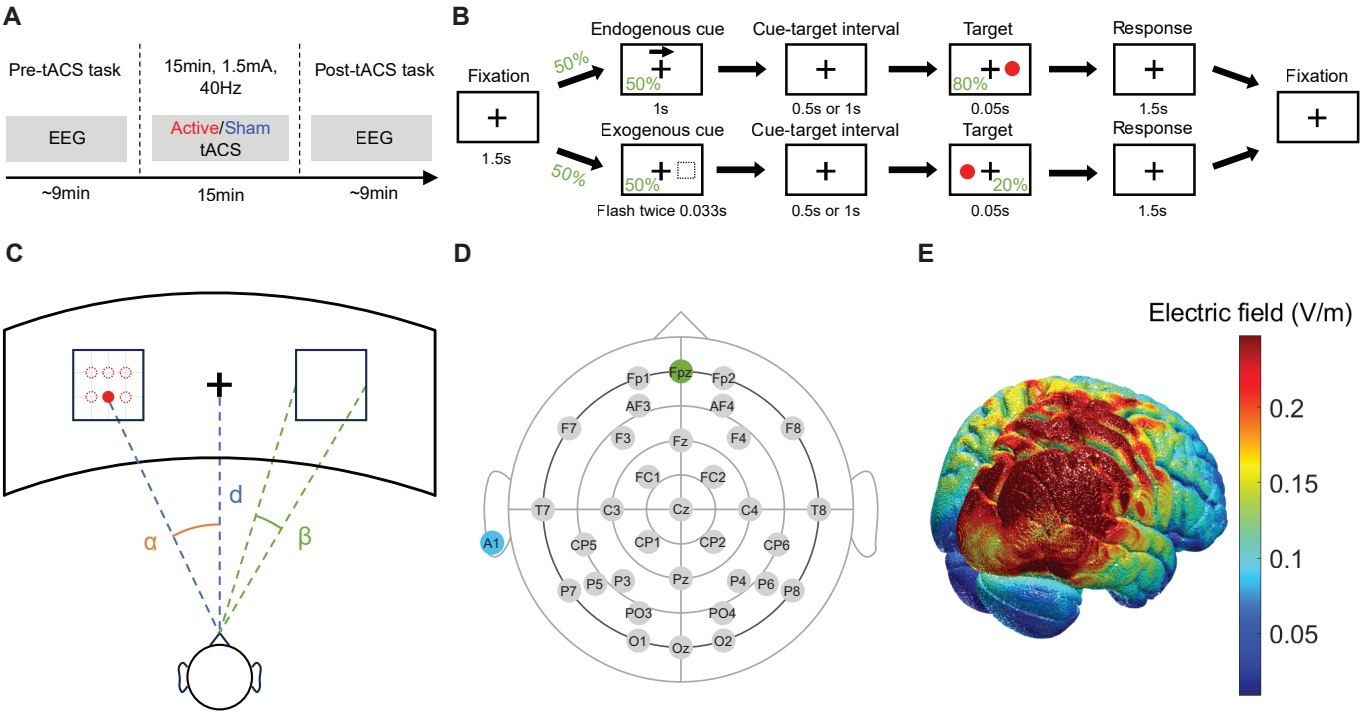

Figure 1. Experiment protocol. (A) Overview of experimental design. (B) Visuo-spatial attention task. (C) Layout of the display and subject in the experiment. (D) Electrode map for EEG. (E) Simulation of the electric field induced by the gamma tACS over the right parieto-occipital region.

Zhang, G., Garrett, D. R., and Luck, S. J. (2023). Optimal filters for erp research i: A general approach for selecting filter settings. bioRxiv doi:10.1101/2023.05.25.542359

Table 1. Contingency table of conditioning and reporting stimulation group

	Report active	Report sham
Condition active	8	2
Condition sham	7	3

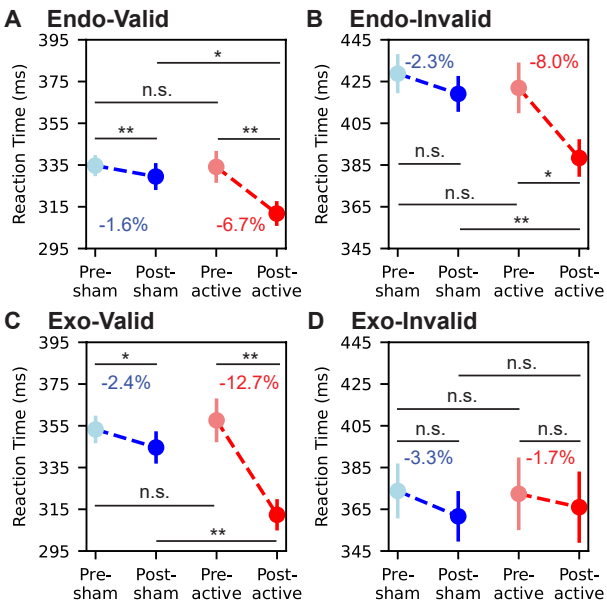

Figure 2. Reaction time change from pre-tACS task to post-tACS task. Trials presenting an endogenous cue followed and a valid target, in which the target appears on the same direction as the cue, is noted as 'Endo-Valid' (A). Same abbreviation rule for 'Endo-Invalid' (B), 'Exo-Valid' (C), and 'Exo-Invalid' (D). Light blue dots, blue dots, light red dots, and red dots denote the mean reaction time of the pre-tACS task of the sham group, the post-tACS task of the sham group, the pre-tACS task of the active group, and the post-tACS task of the active group, respectively. Henceforth we will use the abbreviation for groups and sessions as pre-sham, post-sham, pre-active, and post-active. The vertical lines passing through the dots denote 95%-confidence intervals of the mean reaction time. The percentage number in blue or red colors denotes the pre-post change of the mean reaction time. Four pairwise comparisons are computed to measure the statistical significance, which are: pre-sham and post-sham; pre-active and post-active; pre-sham and pre-active; post-sham and post-active. Pairwise comparisons used t-tests with a Bonferroni correction (*$p<0.05$, **$p<0.01$, n.s., not significant).

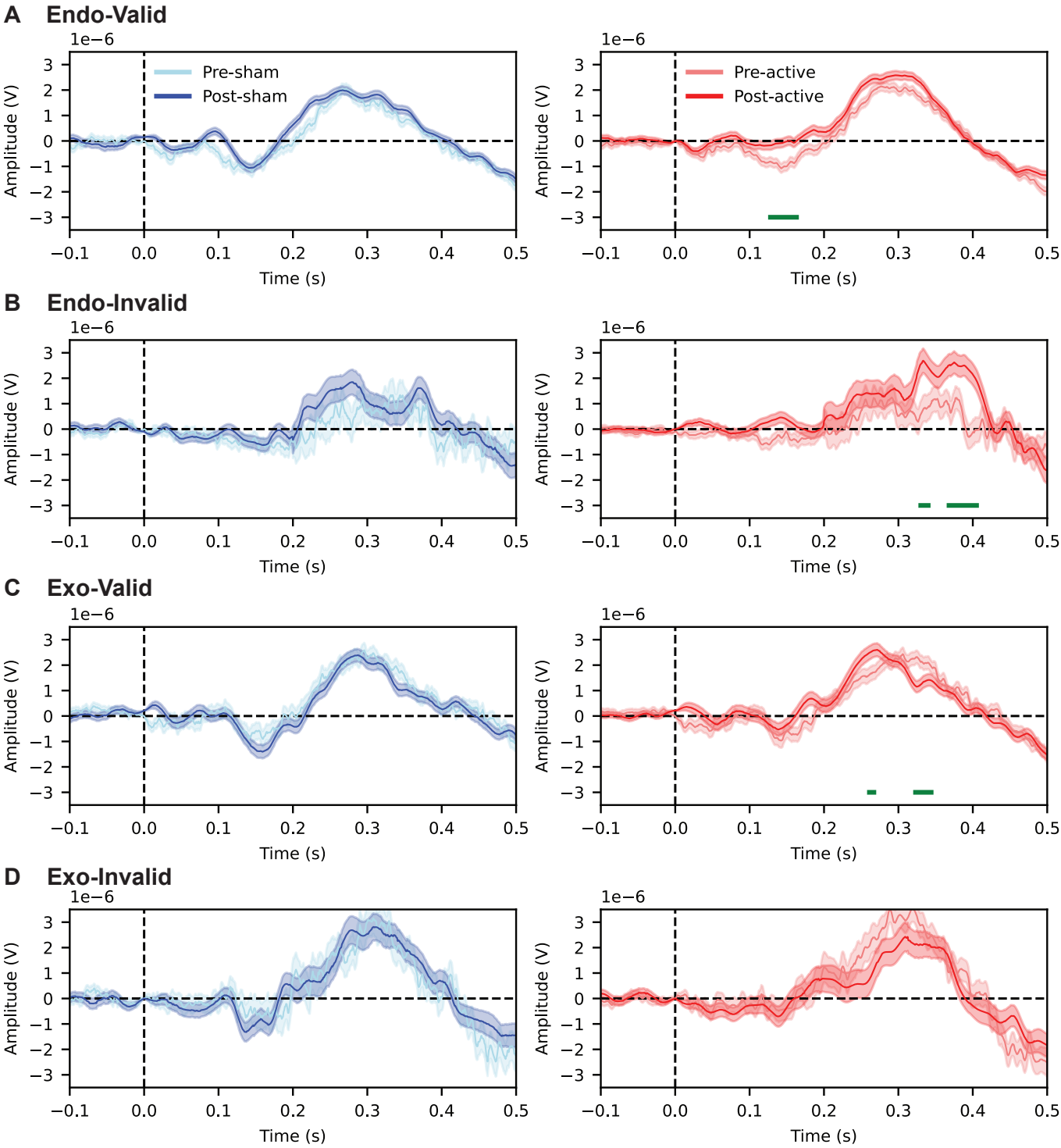

Figure 3. Event-related potential to the onset of targets in tasks. Panels (A)-(D) correspond to four types of trials. From top to bottom: Endo-Valid trials, Endo-Invalid trials, Exo-Valid trials, and Exo-Invalid trials, respectively. Each panel contains two sub-figures: the left sub-figure is the comparison of event-related potential in the pre-sham task and post-sham task, and the right sub-figure is the comparison of event-related potential in the pre-active task and post-active task. Solid color lines in light blue, blue, light red, and red represent the average ERP waveform in pre-sham, post-sham, pre-active, and post-active tasks, respectively. The 0.0 time corresponds to the onset of the target on the screen. The shaded regions along the solid lines reflect the one SEM. Solid green lines along the x-axis represent significant differences in ERPs between pre-tACS and post-tACS ($p<.05$), corrected across time via controlling the false discovery rate (Benjamini and Hochberg (1995)).

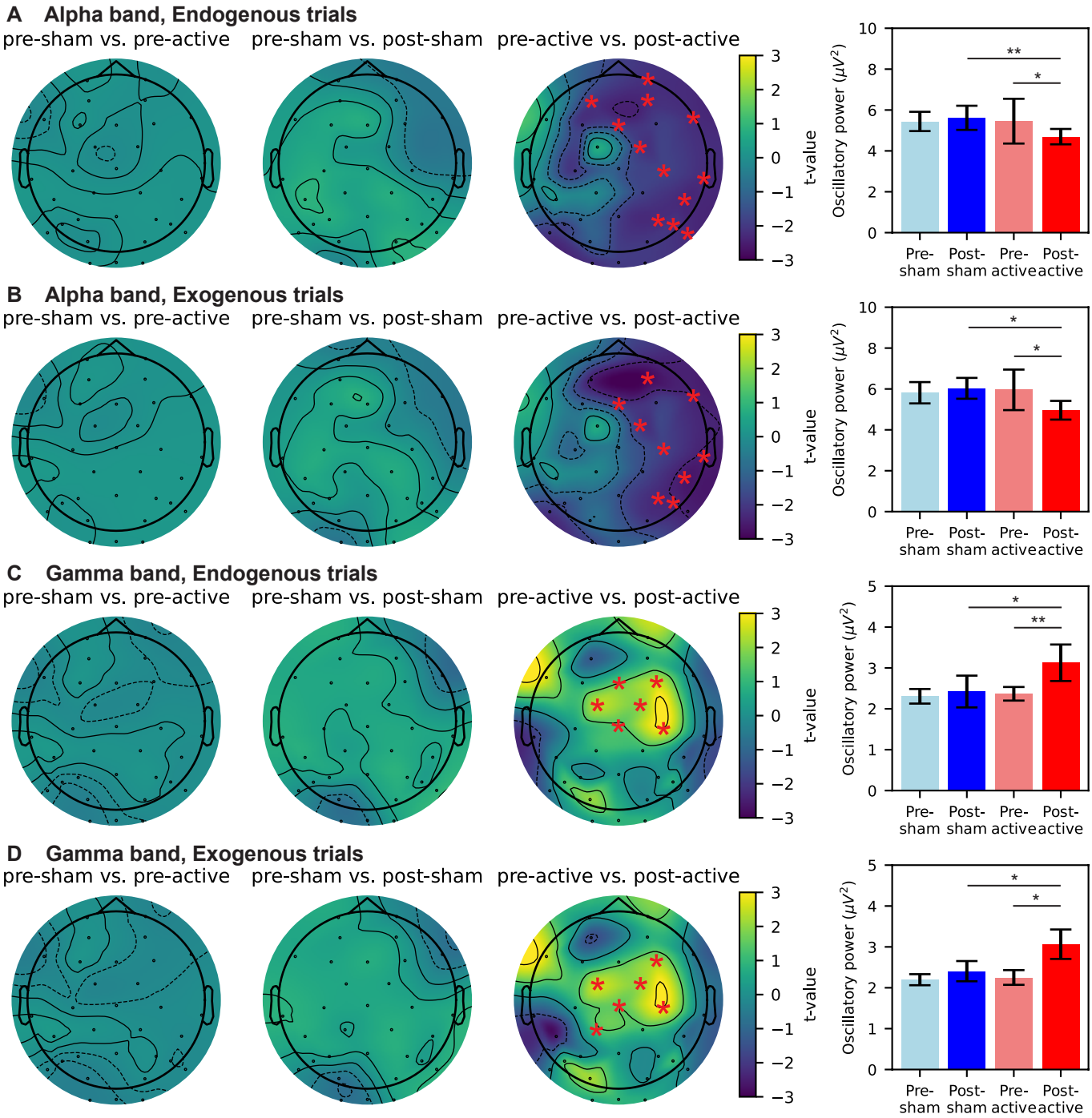

Figure 4. Change of oscillatory power during CTI due to sham/active tACS intervention. Panels from top to bottom represent oscillatory power in the alpha band of endogenous trials (A), alpha band of exogenous trials (B), gamma band of endogenous trials (C), and gamma band of exogenous trials (D), respectively. Topographical maps in each panel from left to right display differences in pre-sham vs. pre-active, pre-sham vs. post-sham, and pre-active vs. post-active, respectively. EEG electrodes forming significant clusters are marked by red stars ($p<.05$). Bar plots reflect the mean oscillatory power of electrodes marked in the corresponding topographical maps. Error bars denote 95%-confidence intervals of the mean oscillatory power. Pairwise comparisons in bar plots use t-tests with a Bonferroni correction (*$p<0.05$, **$p<0.01$).

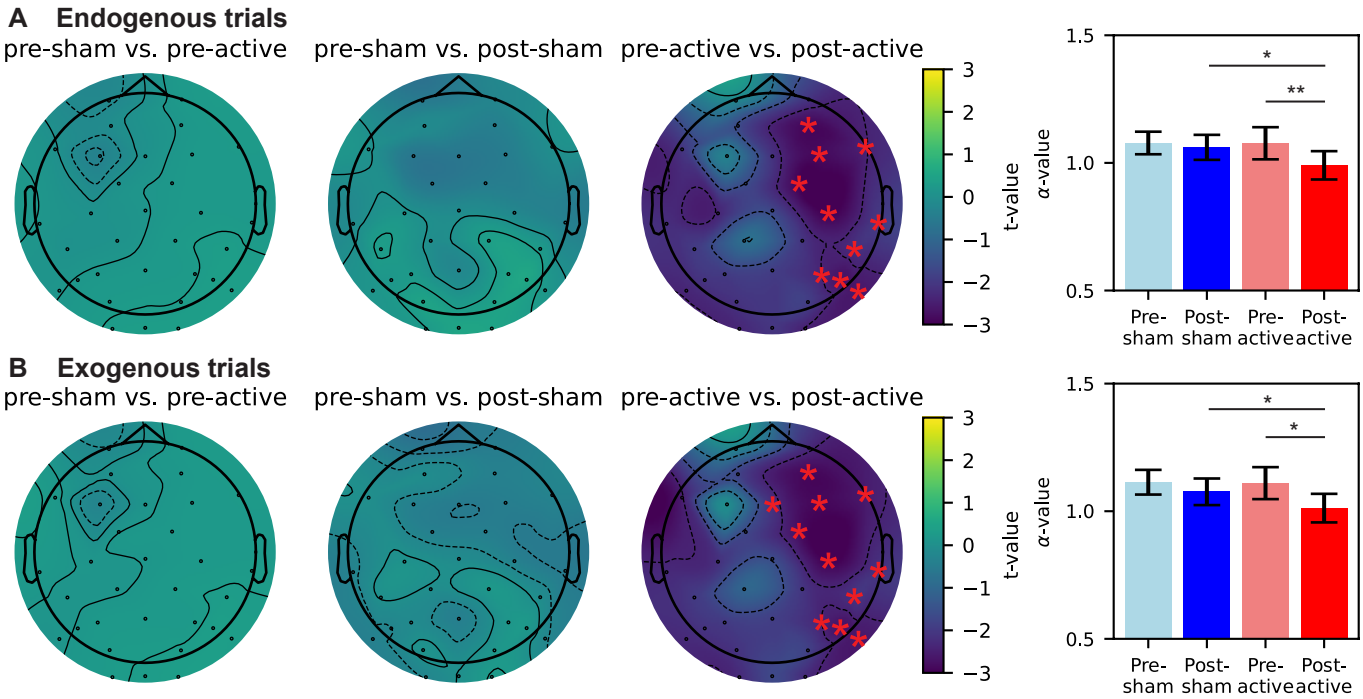

Figure 5. Change of long-range temporal correlations during CTI due to sham/active tACS intervention. (A) Change of α-value in the endogenous trials. (B) Change of α-value in the exogenous trials. Topographical maps in each panel from left to right display differences in pre-sham vs. pre-active, pre-sham vs. post-sham, and pre-active vs. post-active, respectively. EEG electrodes forming significant clusters are marked by red stars ($p<.05$). Bar plots reflect the mean α-value of electrodes marked in the corresponding topographical maps. Error bars denote 95%-confidence intervals of the mean α-value. Pairwise comparisons in bar plots use t-tests with a Bonferroni correction (*$p<0.05$, **$p<0.01$).

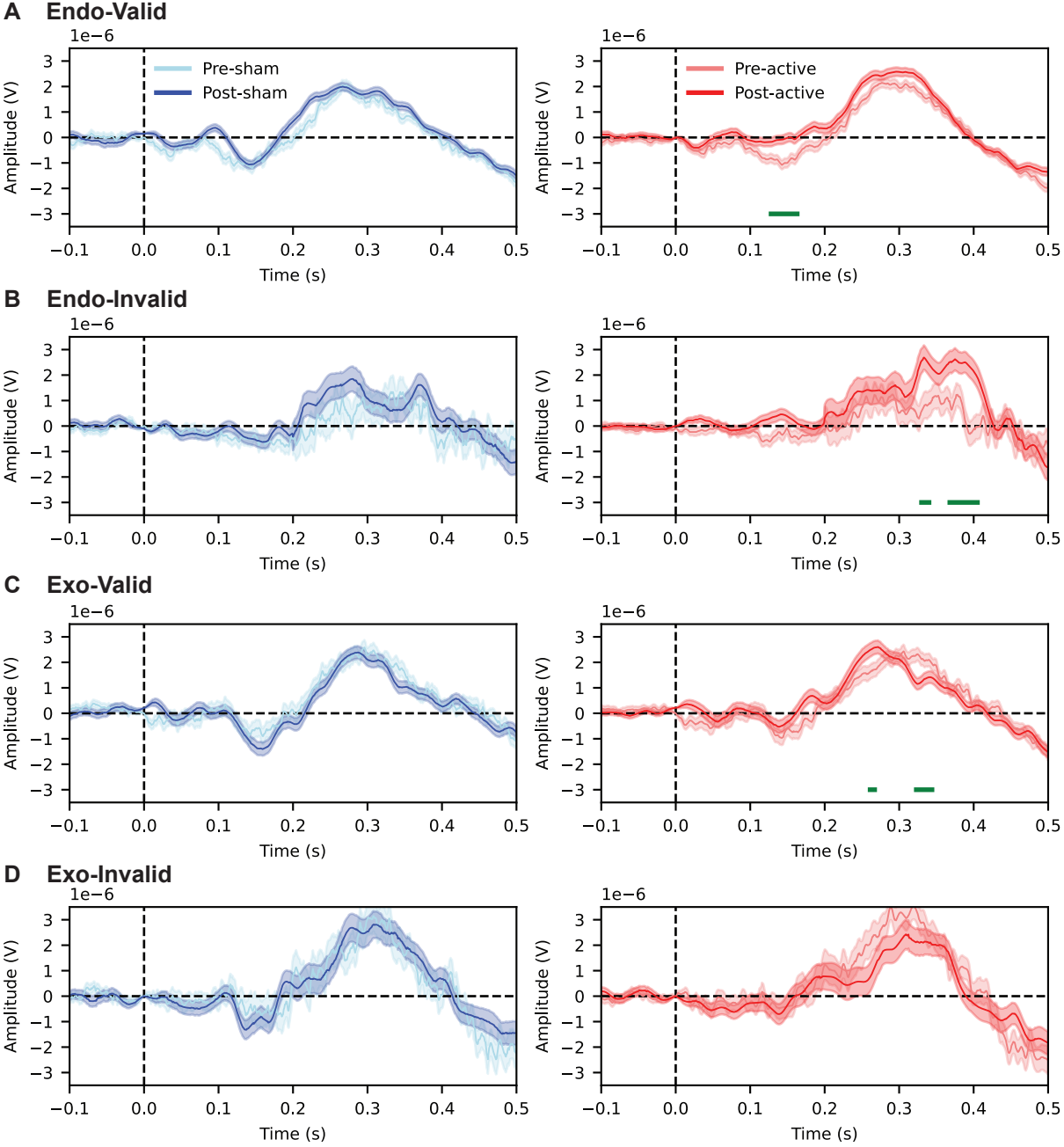
A Endo-Valid
B Endo-Invalid
C Exo-Valid
D Exo-Invalid
1e−6
Pre-sham
Post-sham
Pre-active
Post-active
Amplitude (V)
Time (s)
3
2
1
0
−1
−2
−3
−0.1
0.0
0.1
0.2
0.3
0.4
0.5

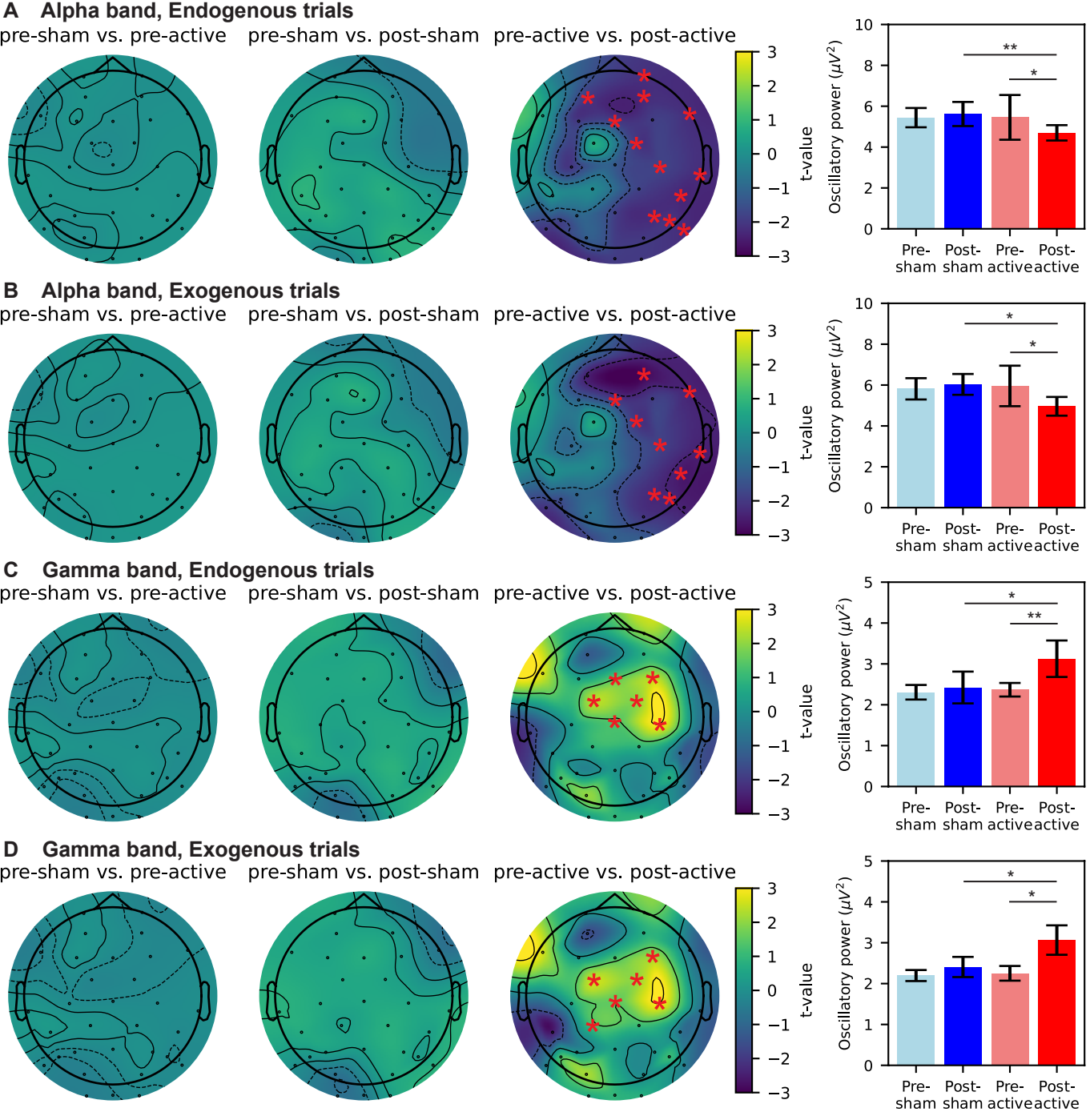
A Alpha band, Endogenous trials
pre-sham vs. pre-active
pre-sham vs. post-sham
pre-active vs. post-active
t-value
Oscillatory power (μV^2)
Pre-sham
Post-sham
Pre-active
Post-active
B Alpha band, Exogenous trials
pre-sham vs. pre-active
pre-sham vs. post-sham
pre-active vs. post-active
t-value
Oscillatory power (μV^2)
Pre-sham
Post-sham
Pre-active
Post-active
C Gamma band, Endogenous trials
pre-sham vs. pre-active
pre-sham vs. post-sham
pre-active vs. post-active
t-value
Oscillatory power (μV^2)
Pre-sham
Post-sham
Pre-active
Post-active
D Gamma band, Exogenous trials
pre-sham vs. pre-active
pre-sham vs. post-sham
pre-active vs. post-active
t-value
Oscillatory power (μV^2)
Pre-sham
Post-sham
Pre-active
Post-active

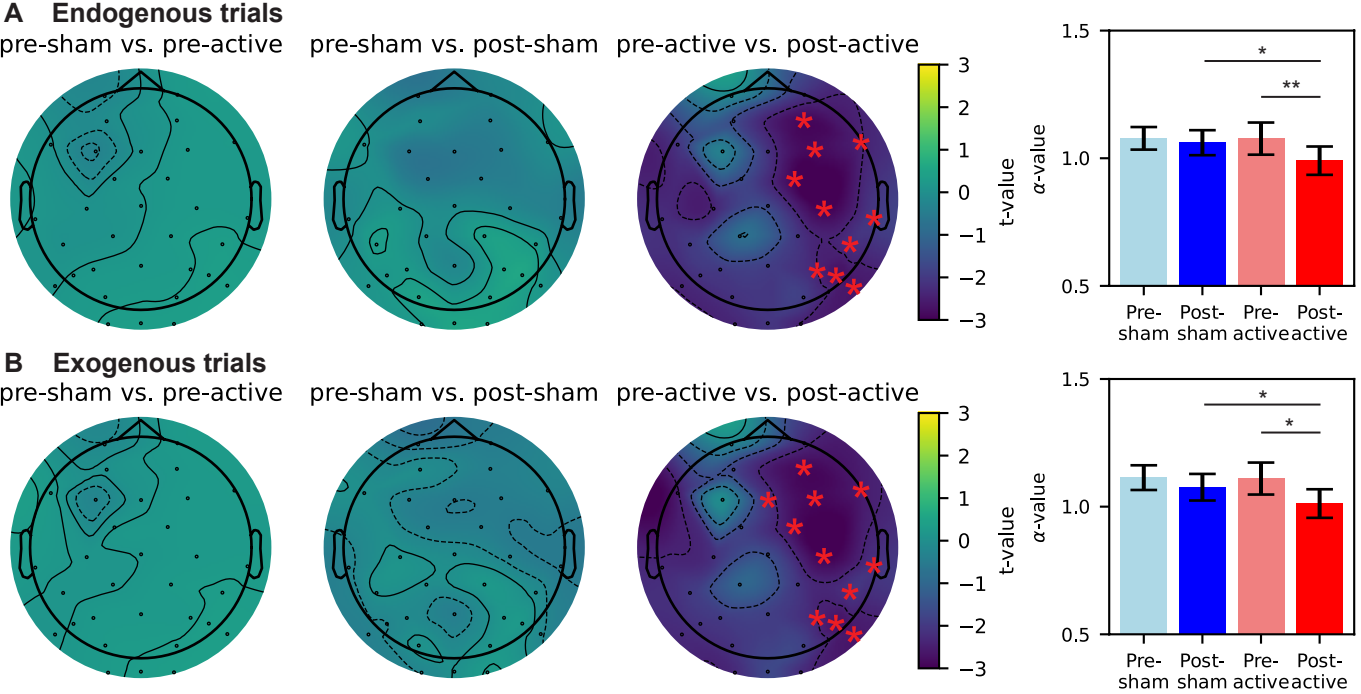
A Endogenous trials
pre-sham vs. pre-active
pre-sham vs. post-sham
pre-active vs. post-active
t-value
3
2
1
0
−1
−2
−3
α-value
1.5
1.0
0.5
*
**
Pre-sham
Post-sham
Pre-active
Post-active
B Exogenous trials
pre-sham vs. pre-active
pre-sham vs. post-sham
pre-active vs. post-active
t-value
3
2
1
0
−1
−2
−3
α-value
1.5
1.0
0.5
*
*
Pre-sham
Post-sham
Pre-active
Post-active

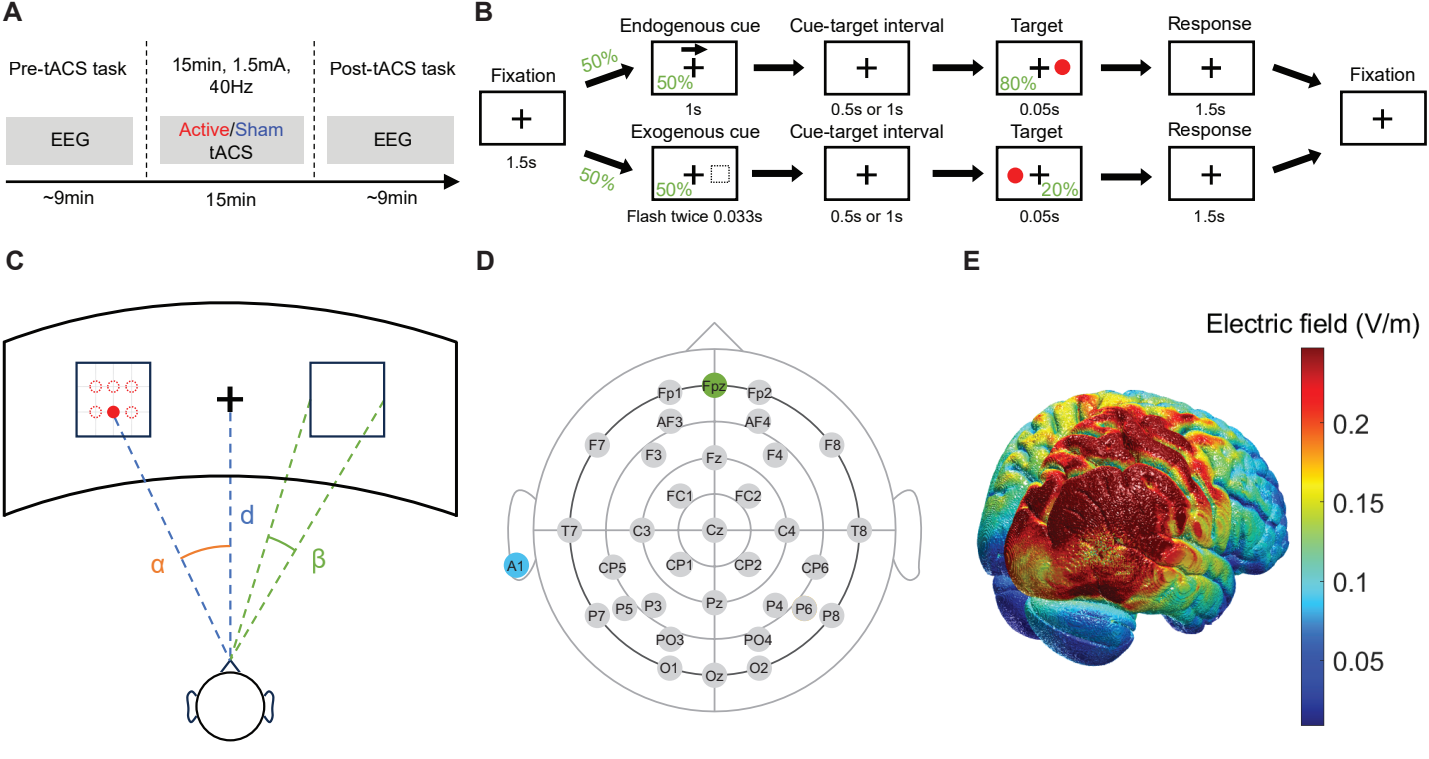
A
Pre-tACS task
15min, 1.5mA, 40Hz
Post-tACS task
EEG
Active/Sham tACS
EEG
~9min
15min
~9min
B
Fixation
1.5s
50%
Endogenous cue
50%
1s
Cue-target interval
0.5s or 1s
Target
80%
0.05s
Response
1.5s
Fixation
50%
Exogenous cue
50%
Flash twice 0.033s
Cue-target interval
0.5s or 1s
Target
20%
0.05s
Response
1.5s
C
d
α
β
D
Fpz
Fp1
Fp2
AF3
AF4
F7
F3
Fz
F4
F8
FC1
FC2
T7
C3
Cz
C4
T8
A1
CP5
CP1
CP2
CP6
P7
P5
P3
Pz
P4
P6
P8
PO3
PO4
O1
Oz
O2
E
Electric field (V/m)
0.2
0.15
0.1
0.05

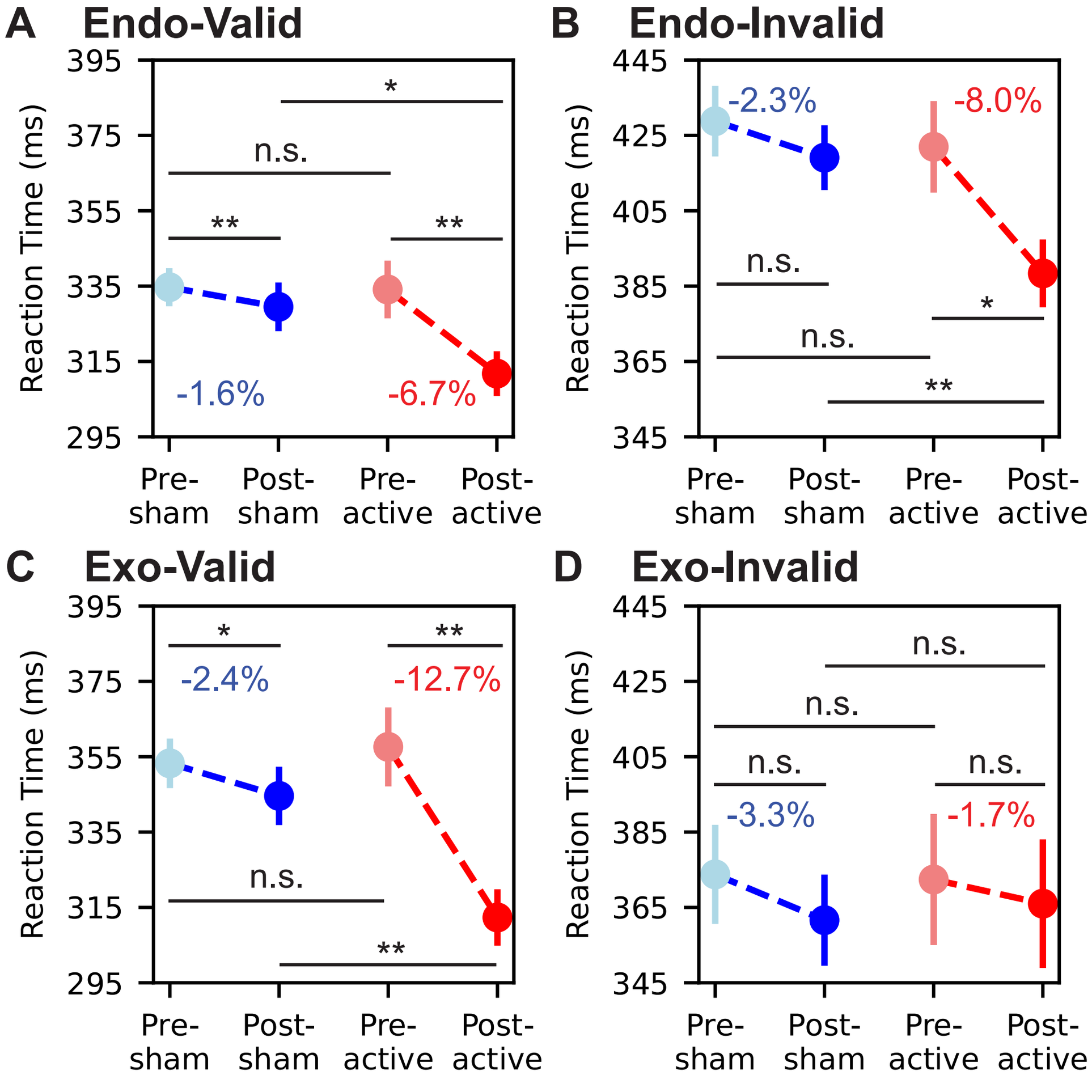
A
Endo-Valid
Reaction Time (ms)
395
375
355
335
315
295
*
n.s.
**
**
-1.6%
-6.7%
Pre-sham
Post-sham
Pre-active
Post-active
B
Endo-Invalid
Reaction Time (ms)
445
425
405
385
365
345
-2.3%
-8.0%
n.s.
*
n.s.
**
Pre-sham
Post-sham
Pre-active
Post-active
C
Exo-Valid
Reaction Time (ms)
395
375
355
335
315
295
*
**
-2.4%
-12.7%
n.s.
**
Pre-sham
Post-sham
Pre-active
Post-active
D
Exo-Invalid
Reaction Time (ms)
445
425
405
385
365
345
n.s.
n.s.
n.s.
n.s.
-3.3%
-1.7%
Pre-sham
Post-sham
Pre-active
Post-active